Channel Estimation Strategies for Coded MIMO Systems

Rose Trepkowski

Thesis submitted to the faculty of the
Virginia Polytechnic Institute and State University
in partial fulfillment of the requirements for the degree of

Master of Science
in
Electrical Engineering

Dr. Brian D. Woerner, Chair
Dr. R. Michael Buehrer
Dr. Gary S. Brown

June 2004
Blacksburg, Virginia

Keywords: MIMO, Quasi-Static Fading, Channel Estimation, V-BLAST

Channel Estimation Strategies for Coded MIMO Systems

Rose Trepkowski

Committee Chairman: Dr. Brian Woerner

Abstract

High transmission data rate, spectral efficiency, and reliability are necessary for future wireless communications systems. In a multipath-rich wireless channel, deploying multiple antennas at both the transmitter and receiver achieves high data rate, without increasing the total transmission power or bandwidth. When perfect knowledge of the wireless channel conditions is available at the receiver, the capacity has been shown to grow linearly with the number of antennas. However, the channel conditions must be estimated since perfect channel knowledge is never known *a priori*. In practice, the channel estimation procedure can be aided by transmitting pilot symbols that are known at the receiver. System performance depends on the quality of channel estimate, and the number of pilot symbols. It is desirable to limit the number of transmitted pilot symbols because pilot symbols reduce spectral efficiency.

This thesis analyzes the system performance of coded multiple-input multiple-output (MIMO) systems for the quasi-static fading channel. The assumption that perfect channel knowledge is available at the receiver must be removed, in order to more accurately examine the system performance. Emphasis is placed on developing channel estimation strategies for an iterative Vertical Bell-Labs Layered Space Time (V-BLAST) architecture. The channel estimate can be sequentially improved between successive iterations of the iterative V-BLAST algorithm. For both the coded and uncoded systems, at high signal to noise ratio only a minimum number of pilot symbols per transmit antenna are required to achieve perfect channel knowledge performance.

Acknowledgements

I would like to express my sincerest appreciation towards my advisor, Dr. Brian Woerner. In addition to being a great source of knowledge and encouragement, he has always believed in me. I am grateful to Dr. R. Michael Buerher and Dr. Gary Brown for taking the time to serve on my thesis committee.

On a personal note, I would like to thank my colleague, Kris Hall for many helpful discussions. I would like to thank my Mother, Beth, and my sisters, Martha and Lisa, for all their love, understanding and encouragement. Finally, I would like to thank my husband, Jerry, for being involved with so many aspects of my thesis-including help with editing. I would like to thank him for all of his love, help, motivation and patience during my academic career, and always. Without my family, my success would not be possible.

Contents

List of Figures

List of Tables

Chapter 1

Introduction

1.1 Overview

High transmission data rate, spectral efficiency, and reliability are necessary for future wireless communications systems. Unlike Gaussian channels, wireless channels suffer from attenuation due to multipath in the channel. Multiple copies of a single transmission arrive at the receiver at slightly different times. Without diversity techniques, severe attenuation makes it difficult for the receiver to determine the transmitted signal. Diversity techniques provide potentially less-attenuated replica(s) of the transmitted signal at the receiver.

Multiple-Input Multiple-Output (MIMO) antenna systems are a form of spatial diversity. In a multipath-rich wireless channel, deploying multiple antennas, at both the transmitter and receiver, achieves high data rate without increasing the total transmission power or bandwidth. Additionally, the use of multiple antennas at both the transmitter and receiver provides significant increase in capacity [1].

When perfect channel knowledge is available at the receiver, the capacity has been shown to grow linearly with the number of antennas. Most MIMO detection schemes are based on perfect channel knowledge being available at the receiver. However, perfect channel knowledge is never known *a priori*. In practice, the channel estimation procedure is aided by transmitting pilot symbols that are known at the receiver. Pilot symbols reduce spectral efficiency. The system performance depends on the quality of the channel estimate. The quality of the channel estimate is dependent on the number of pilot

symbols. To increase spectral efficiency, it is desirable to limit the number of transmitted pilot symbols.

MIMO systems are ideal for rich scattering environments. The channel between any pair of transmit and receive antennas can be modeled as independent identically distributed (i.i.d.) complex Gaussian random variables when there are significant number of multipaths in the environment. Possible occurrences of the idealized channel conditions include the class of indoor channels, such as wireless local area networks, fixed wireless networks, and wireless ad-hoc networks.

1.2 Outline

This thesis discusses three dominant MIMO techniques; Space-Time Block Coding (STBC) [2], Space-Time Trellis Coding (STTC) [3], and Vertical-Bell Labs Layered Space Time architecture (V-BLAST) [4]. The scenario under consideration is an indoor wireless local area network. Due to practical size constraints, the number of transmit and receive antennas is kept small; between 2-4 transmit antennas and 1-4 receive antennas. The channel environment is assumed to remain essentially unchanged for lengthy time periods.

This thesis examines the performance of coded MIMO systems for slowly changing channel conditions. It will be shown that some coded MIMO systems can be strongly inhibited in this channel environment. The assumption that perfect channel knowledge is available at the receiver must be removed in order to more accurately examine the system performance. As the number of antennas increase, so does the number of parameters to be estimated. This adds to the complexity involved in obtaining an accurate channel

estimate. Therefore, when evaluating channel estimation strategies, only systems with four transmit and four receive antennas will be considered.

This thesis is organized as follows.

In addition to the introduction and overview, Chapter 1 provides a description of the MIMO channel model. Three different channel models are presented; a quasi-static frequency non-selective fading channel, a quasi-static frequency selective fading channel, and a block fading frequency non-selective channel.

Chapter 2 discusses STBC and STTC systems. A concatenated STBC-TCM system is described and compared against STTC in both the quasi-static and block fading channel environment. The STTC system will be shown to outperform the STBC-TCM system for quasi-static channel environment. However, when the quasi-static channel is changed into a block fading channel, the STBC-TCM outperforms the STTC. Additionally, the performance is examined for different mapping techniques for the STBC-TCM system. The discussion on STBC and STTC provides background information. Previous work has examined channel estimation strategies for STBC and STTC [5] [6] [7].

Chapter 3 describes the original V-BLAST architecture. The performances of several variations of the original V-BLAST detection algorithm are compared against each other. Additionally, the perfect channel knowledge assumption is removed. Least Squares and MAP estimation are used to estimate the unknown channel parameters.

Chapter 4 examines coded V-BLAST systems. Convolutional coding is combined with the original V-BLAST systems described in Chapter 3. The performance potential of the coded V-BLAST system is limited by the lack of diversity in the quasi-static channel. As with the STBC-TCM system, the performance of the coded V-BLAST system

improves when the channel is block fading. Instead of transforming the channel model, another solution is to change the detection procedure of the V-BLAST system. Combining a previously proposed iterative V-BLAST algorithm [8] with convolutional coding yields performance improvements over the uncoded system. Finally, a coded V-BLAST-OFDM architecture is proposed for the frequency selective quasi-static channel. The proposed architecture yields good performance for both V-BLAST detection algorithms.

Chapter 5 focuses on channel estimation strategies for the iterative V-BLAST system, described in Chapter 4. A minimum number of pilot symbols are transmitted to assist in the channel estimation process. This limits the decrease in spectral efficiency. An initial channel estimate can be improved, between iterations of the iterative V-BLAST algorithm, using a previously proposed channel estimator [6]. Some simple extensions will be proposed to yield nearly perfect channel knowledge performance at high signal to noise ratio. Different techniques are proposed for the coded and uncoded iterative V-BLAST systems.

1.3 The MIMO Channel

Multiple-Input Multiple-Output (MIMO) systems yield vast capacity increases when the rich scattering environment is properly exploited [1]. When examining the performance of MIMO systems, the MIMO channel must be modeled properly. The MIMO channel models used throughout this thesis are described in this section. The primary MIMO channel model under consideration is the quasi-static, frequency non-selective, Rayleigh fading channel model. Figure 1.1 shows a block diagram of a MIMO system with N_t

transmit antennas and N_r receive antennas. The channel for a MIMO system can be represented by

$$H = \begin{bmatrix} h_{11} & \cdots & h_{1N_t} \\ h_{21} & \cdots & h_{2N_t} \\ \vdots & \ddots & \vdots \\ h_{N_R 1} & \cdots & h_{N_r N_t} \end{bmatrix} \tag{1.1}$$

where h_{ij} is the complex channel gain between transmitter *j* and receiver *i*. Each channel gain h_{ij} is assumed to be independently identically distributed (i.i.d) zero mean complex Gaussian random variables with unit variance [1].

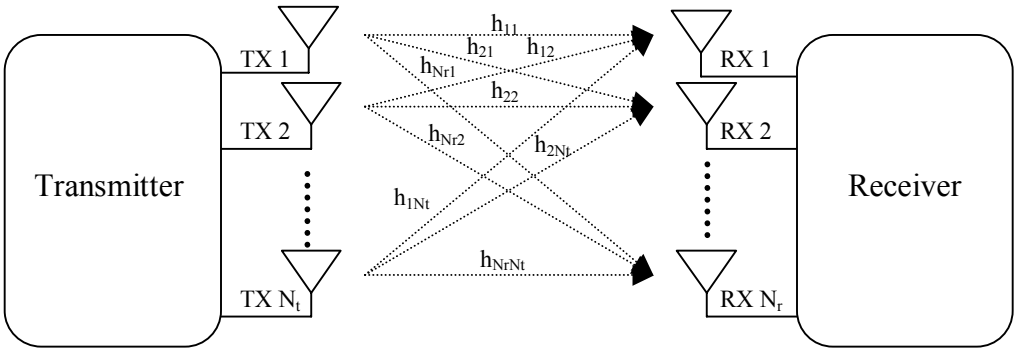

Figure 1.1 MIMO Channel

Under the quasi-static assumption, the channel remains constant over the length of a frame, changing independently between consecutive frames. When the antenna elements are spaced sufficiently apart (at least half a wavelength, for indoor applications) and there are enough scatterers present that the received signal at any receive antenna is the sum of several multipath components, the channel paths are modeled as independent and uncorrelated. The channel undergoes frequency non-selective fading when the coherence bandwidth of the channel is large compared to the bandwidth of the transmitted signal [10].

1.3.1 Frequency Selective Fading

MIMO channels are often frequency selective. The channel undergoes frequency-selective fading when the coherence bandwidth of the channel is small compared to the bandwidth of the transmitted signal [10]. When the channel is modeled as frequency selective fading, individual frequencies are attenuated and faded differently. Frequency selective fading channels occur when the multi-path delay is significant, relative to the symbol period. The symbols will overlap, resulting in intersymbol interference. The transmitted signal is severely attenuated and delayed by the channel. As a result, the received signal consists of multiple versions of the transmitted signal. The received signal is a linear combination of the current symbols and previous symbols.

The frequency selective channel can be modeled as a FIR filter with memory length *L*. The channel between transmitter *j* and receiver *i* is given by

$$h_{i,j}(\tau) = \sum_{l=1}^{L} \alpha_{i,j}^{(l)} \delta\left(t - \tau_{t,j}^{(l)}\right) \tag{1.2}$$

where for the lth path, $\alpha_{i,j}$ is the complex channel gain and $\tau_{t,j}$ is the delay of the l^{th} path. The channel gain between different transmit and receive antennas is assumed to be i.i.d.

1.3.2 Block Fading

Most of the work considered in this thesis uses the quasi-static channel model. However, block fading is considered for comparison purposes. A quasi-static channel can be transformed into a block fading channel based by manipulating the data at the transmitter and receiver. The channel is still modeled as quasi-static, frequency non-selective, Rayleigh fading. Figure 1.2 illustrates the concept of block fading. The channel is still

considered constant over a frame, but data transmitted across N consecutive frames form a block [11]. Within each block, the data is interleaved across the frames. Block fading results in increased decoding delay. However, if the block length is long enough, consecutive symbols at the decoder will have undergone completely different fading. The block fading channel allows for symbols affected by a deep fade to be distributed across time, thus protecting against burst errors.

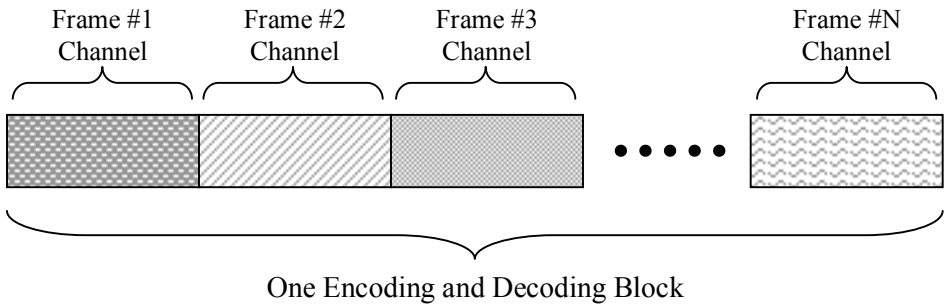

Figure 1.2 Block Fading Channel Model

Chapter 2

Space-Time Coding

2.1 Introduction

Space-time coding introduces redundancy in space, though the addition of multiple antennas, and redundancy in time, through channel coding. Two prevailing space-time coding techniques are Space Time Block Codes (STBC) and Space Time Trellis Codes (STTC). STBC provide diversity gain, with very low decoding complexity, whereas STTC provide both diversity and coding gain at the cost of higher decoding complexity. STBC must be concatenated with an outer code to provide coding gain. Concatenating STBC with Trellis Coded Modulation (TCM) creates a bandwidth efficient system with coding gain.

This chapter first explains the decoding procedure for STBC with two or three transmit antennas. Next, the system model and decoding procedure is introduced for the concatenated STBC-TCM system. The performance of the concatenated systems is examined under the quasi-static and block fading channel conditions. Additionally, the performance of the concatenated system is evaluated for three different mapping techniques. Finally, STTC are compared against the concatenated STBC-TCM scheme for the quasi-static and block fading channel.

2.2 Space Time Block Coding

Space Time Block Coding is a low complexity, transmit diversity scheme that yields the same diversity advantage as maximal ratio combining. Originally proposed by Alamouti,

as a full rate code for two transmit antennas [2], STBC now extends to an arbitrary number of transmit antennas and varying code rates [12]. Figure 2.1 shows the system diagram for the original Alamouti STBC with two transmit antennas and one receive antenna. Additional receive antennas allow the system to benefit from receive diversity.

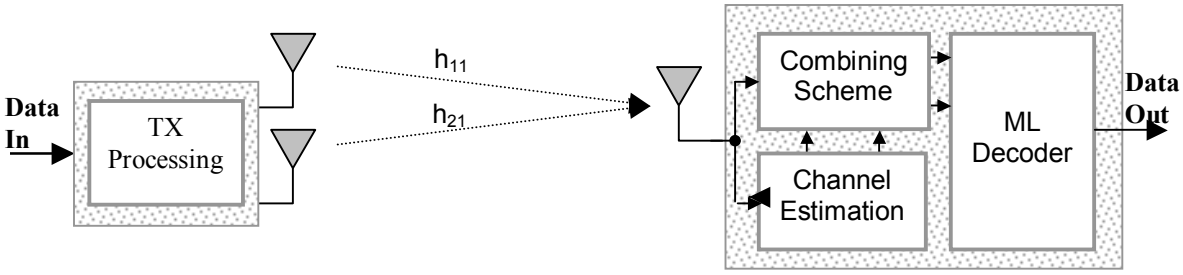

Figure 2.1 Alamouti STBC System Diagram

Table 2.1 summarizes the details of two orthogonal STBC; a two transmit antenna code (G2), and a three transmit antenna code (H3). The encoding procedure is illustrated by the transmission matrices G2 and H3. The rows of the matrices G2 and H3 represent the simultaneously transmitted symbols from each of the transmit antennas. The columns correspond to the time interval for which the symbol is transmitted.

Table 2.1 STBC Transmission Matrices

G2	H3
Code rate = 1	Code rate = ¾
$G_2 = \begin{pmatrix} x_1 & x_2 \\ -x_2^* & x_1^* \end{pmatrix}$	$H_3 = \begin{pmatrix} x_1 & x_2 & \frac{x_3}{\sqrt{2}} \\ -x_2^* & x_1^* & \frac{x_3}{\sqrt{2}} \\ \frac{x_3^*}{\sqrt{2}} & \frac{x_3^*}{\sqrt{2}} & \frac{\left(-x_1 - x_1^* + x_2 - x_2^*\right)}{2} \\ \frac{x_3^*}{\sqrt{2}} & -\frac{x_3^*}{\sqrt{2}} & \frac{\left(x_2 + x_2^* + x_1 - x_1^*\right)}{2} \end{pmatrix}$

STBC Receiver

At time *t*, the received signal at antenna *j*, is given by:

$$r_t^j = \sum_{i=1}^{n} h_{i,j} x_t^i + n_t^j \tag{2.1}$$

In matrix notation, the received signal is represented by:

$$R=Hx+n \tag{2.2}$$

where n is the noise vector and H is the Rayleigh fading channel matrix.

The maximum likelihood detector, shown in Figure 2.1, uses the output of a combiner to make a decision. For the two transmit G2 code, the combining technique for x_1 and x_2 is [2]:

$$\tilde{x}_1 = \sum_{j=1}^{numRx} \left(r_1^j h_{1,j}^* + \left(r_2^j\right)^* h_{2,j} \right) \qquad \tilde{x}_2 = \sum_{j=1}^{numRx} \left(r_1^j h_{2,j}^* - \left(r_2^j\right)^* h_{1,j} \right) \tag{2.3}$$

The combining technique for H3 is given in [12].

2.3 STBC Concatenated with Trellis Coded Modulation

Space Time Block Coding is a simple technique to achieve diversity; however, there is no significant coding gain. An outer channel code is required to yield coding gain. Trellis Coded Modulation (TCM) is a bandwidth efficient technique that combines coding and modulation, without reducing the data rate [13]. Concatenating STBC with TCM provides coding gain with a reasonable increase in complexity. Figure 2.2 shows the block diagram for the concatenated system. First, the TCM encoder encodes the source data. Next, the encoded data is interleaved, and then mapped according to the desired signal constellation. Finally, the space-time encoder encodes the data. At each time

interval, the symbols are modulated and transmitted simultaneously over different transmit antennas.

At the receiver, the received data is combined according to the combining techniques described for STBC. The soft output of the combiner is sent directly to the detiniterleaver. Finally, a TCM decoder, such as the Viterbi algorithm, decodes the data.

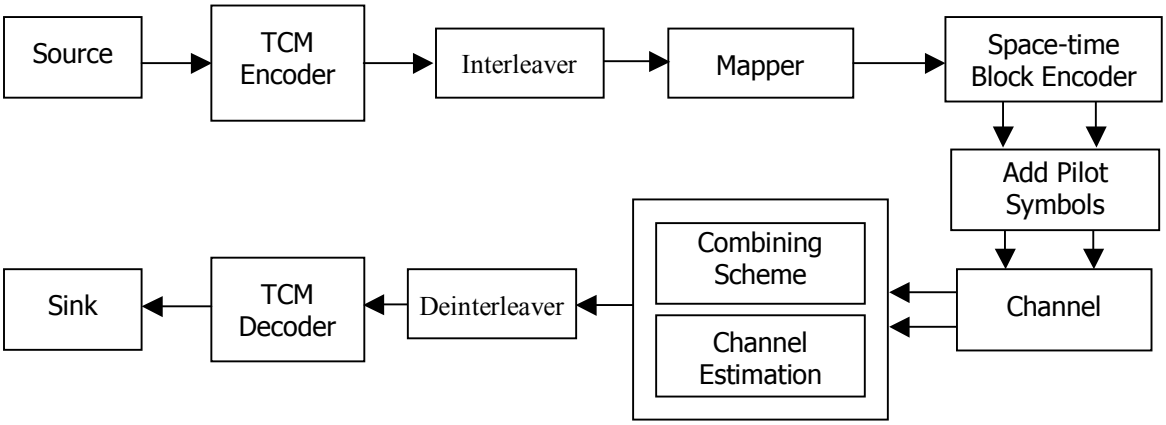

Figure 2.2 System Diagram of Concatenated STBC –TCM

Two different TCM codes were evaluated for concatenation with STBC: a rate 2/3 eight state code, and a rate 2/3 sixteen state code. Previous work has shown that for Rayleigh fading, the optimal sixteen and eight state TCM codes are the original Ungerboeck codes [14]. Therefore, the only TCM codes implemented were the Ungerboeck codes [13].

8PSK modulation was used for the concatenated system. Figure 2.3 shows three different 8PSK mapping techniques. Figure 2.3 (a) shows the Ungerboeck set partitioning mapping. Figure 2.3 (b) shows Gray coded mapping. Figure 2.3 (c) shows the V-mapper. The V-mapper combines set partitioning and Gray coded mapping [15]. The set partitioning and V-mapper constellations obey the design rules, based on the maximization of Euclidean distance, originally described by Ungerboeck [13]. On the other hand, the Gray coded mapping is based on the maximization of free distance. Gray

coding was considered because it typically yields better BER performance than natural mapping (such as set partitioning).

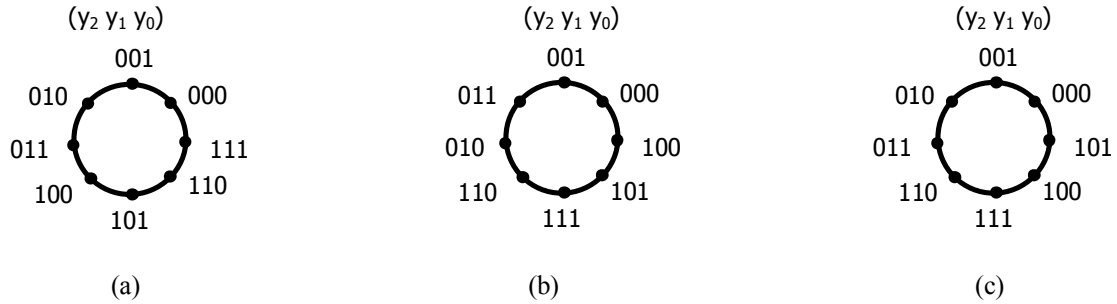

Figure 2.3 Mapping Techniques. (a) Set Partitioning. (b) Gray. (c) V-Mapper.

Figure 2.4 shows simulation results for the STBC-TCM system with the three mapping techniques. The quasi-static channel is constant over the length of the codeword. Figure 2.4 (a) shows the BER for STBC G2 concatenated with the sixteen state code. Figure 2.4 (b) shows the BER for STBC H3 concatenated with the eight state code. Figure 2.4 (c) shows the frame error rate (FER) for STBC G2 concatenated with the sixteen state code. Figure 2.4 (d) shows the FER for STBC H3 concatenated with the eight state code. Additionally, figure 2.4 shows the performance of the uncoded STBC system. For both concatenated systems, the Gray mapping leads to the best BER performance. However, set-partitioning leads to the best FER performance. Concatenating TCM with STBC does not improve the BER performance for the quasi-static channel. However, the STBC-TCM does provide better FER performance than the uncoded STBC. This indicates that when a frame is in error, there are many bits in error. When the channel is constant over the length of the codeword, there is not always enough diversity present in the channel. The TCM decoder limits the BER performance for the quasi-static channel.

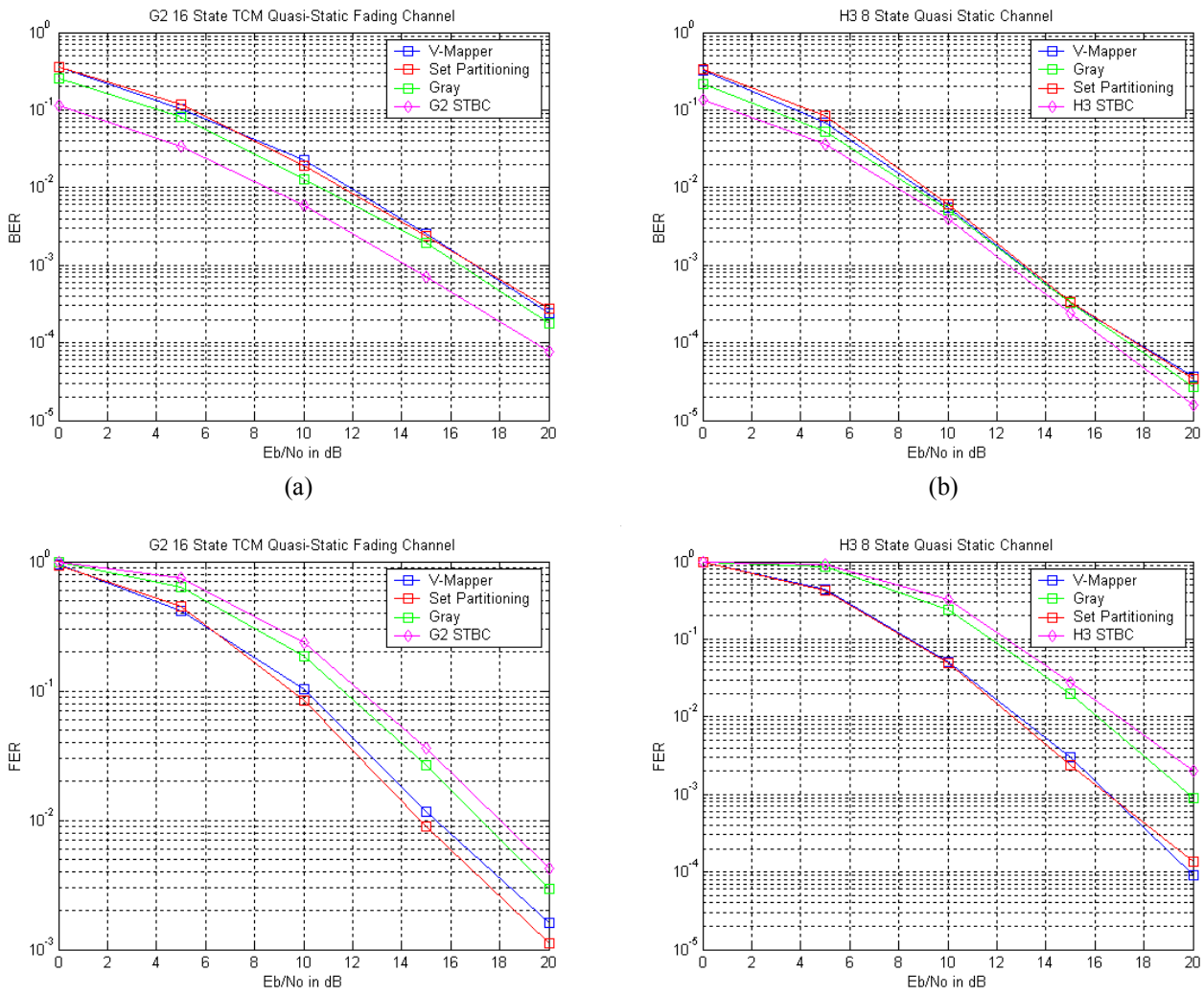

Figure 2.4 STBC-TCM systems for the quasi-static channel. (a) BER G2 concatenated with 16 state code. (b) BER H3 concatenated with eight state code. (c) FER G2 concatenated with 16 state code. (d) FER H3 concatenated with eight state code.

Figure 2.5 shows the results of the above concatenated systems for the block fading channel model. Figure 2.5 (a) shows the BER for the STBC G2 concatenated with the sixteen state code. Figure 2.5 (b) shows the BER for the STBC H3 concatenated with the eight state code. Figure 2.5 (c) shows the FER for the STBC G2 concatenated with the sixteen state code. Figure 2.5 (d) shows the FER for the STBC H3 concatenated with the eight state code. For the block fading channel model, set-partitioning and the V-mapper

lead to better BER and FER than Gray mapping. Furthermore, for the block-fading channel model, all mapping techniques outperform the uncoded STBC system.

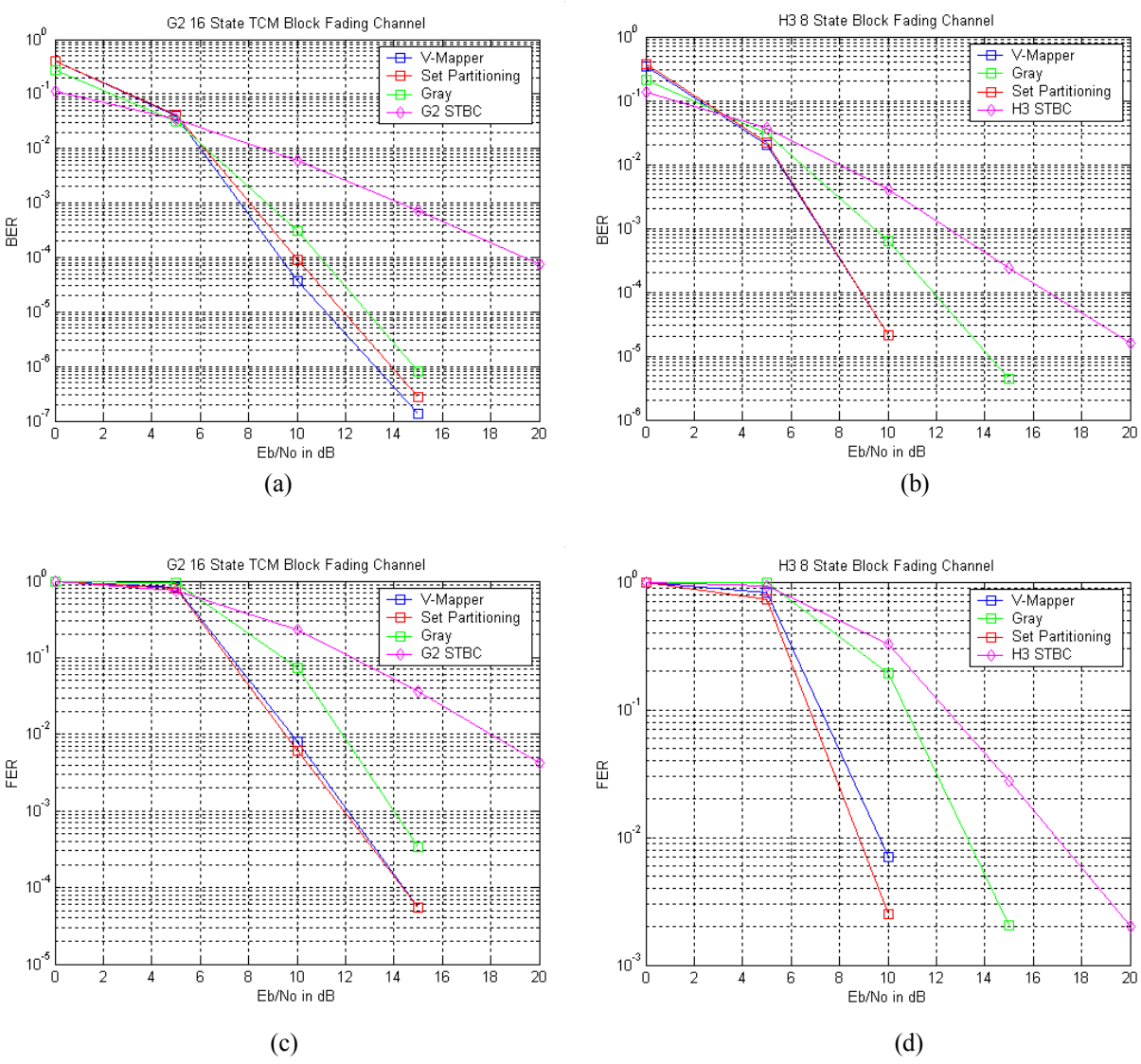

Figure 2.5 STBC-TCM systems for the block fading channel. (a) BER G2 concatenated with 16 state code (b) BER H3 concatenated with eight state code (c) FER G2 concatenated with 16 state code (d) FER H3 concatenated with eight state code

2.4 Space Time Trellis Coding

Space Time Trellis Coding (STTC) is a MIMO technique that provides full diversity and coding gain [3]. STTC combines coding, modulation, transmit diversity, and optional

receive diversity. The coding gain is obtained at the cost of increased decoding complexity. Originally proposed for two transmit antennas, STTC has since been extended to more transmit antennas [16], [17]. Figure 2.6 shows a block diagram of a STTC, with N_t transmit antennas and N_r receive antennas. First, the channel code encodes the source data. The space-time trellis encoder maps one symbol at a time, to an N_t *x 1* vector output. The channel code creates correlation between codewords across time (between successive symbols) and space (between different transmit antennas).

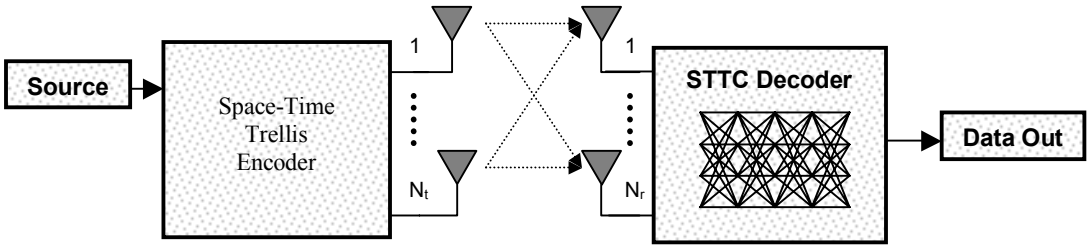

Figure 2.6 Block Diagram of STTC

At the receiver, the implemented STTC decoder is the Viterbi algorithm. As the number of states increase, the BER performance improves at the cost of additional decoding complexity. Assuming perfect channel knowledge is available at the receiver, the branch metric is given by

$$\sum_{j=1}^{N_r}\left|r_t^j - \sum_{j=1}^{N_r} h_{j,i} q_t^i\right|^2 \tag{2.4}$$

where at time *t*, r_t^j is the received signal at the jth receive antenna, $h_{j,i}$ is the channel path between transmit antenna *i* and receive antenna *j*, and $q_t^1 q_t^1 \cdots q_t^n$ corresponds to the transition through the trellis.

2.5 STTC, STBC+TCM Comparison

The structure of Space Time Block Coding concatenated with Trellis Coded Modulation is similar to that of Space Time Trellis Coding. Previous work has shown that STBC-TCM outperforms STTC [18]. However, they did not consider the case where the channel is constant over the length of the codeword. In this section, the performances for both the STBC-TCM and STTC systems will be compared for the quasi-static and block fading channel models. The two schemes compared have the same spectral efficiency, trellis complexity, code rate, and number of transmit and receive antennas.

The systems under consideration have two transmit antennas; however, this is easily extendable to include more transmit antennas. G2 is the STBC implemented in the STBC-TCM system. Figure 2.7 shows the trellis diagrams for the eight and sixteen state trellis codes. The transmitted symbols for the STTC are to the left of each trellis diagram. The symbols correspond to the QPSK constellation, shown in Figure 2.7 (c). The first symbol shown is the symbol transmitted by the first transmit antenna; the second is the symbol transmitted by the second transmit antenna. The encoded symbols for the TCM are to the right of each trellis diagram. The symbols correspond to 8PSK mapping, shown in Figure 2.3.

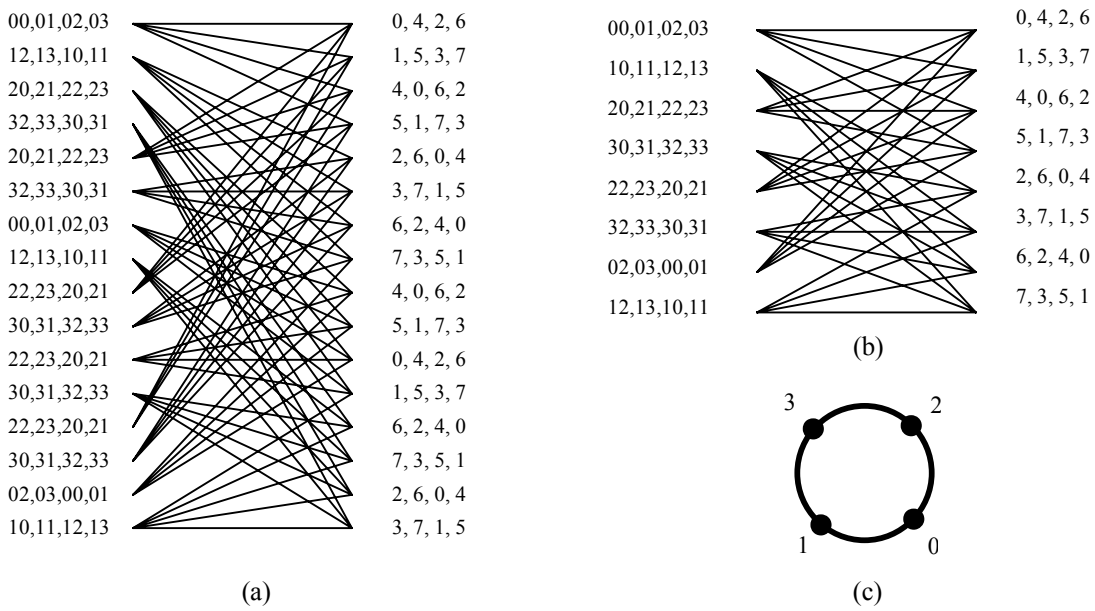

Figure 2.7 Trellis Diagrams. (a) 16 State Codes, (b) Eight State Codes, (c) QPSK Constellation.

Figure 2.8 shows a comparison between the frame error rate (FER) for STTC and STBC-TCM. The channel is block fading, with perfect channel knowledge available at the receiver. Set-partitioning is the mapping technique implemented for the STBC-TCM. The STBC-TCM outperforms STBC for both cases considered (eight and sixteen states).

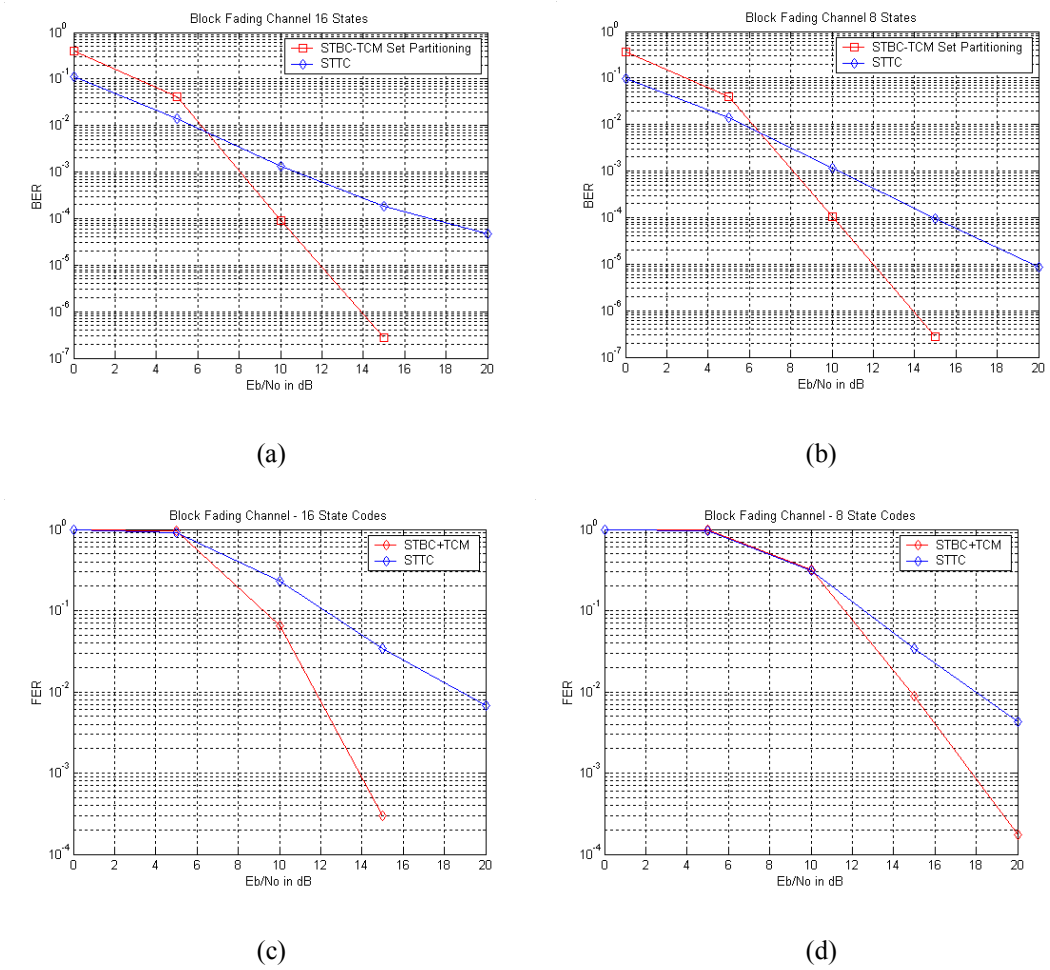

Figure 2.8 STTC compared with STBC-TCM for the block fading channel. (a) BER 16 State (b) BER 8 State (c) FER 16 State (d) FER 8 State.

Figure 2.9 shows a comparison between STTC and STBC-TCM for the quasi-static channel. For all cases, STTC yields better BER performance. Interleaving does not provide enough diversity to distribute burst errors.

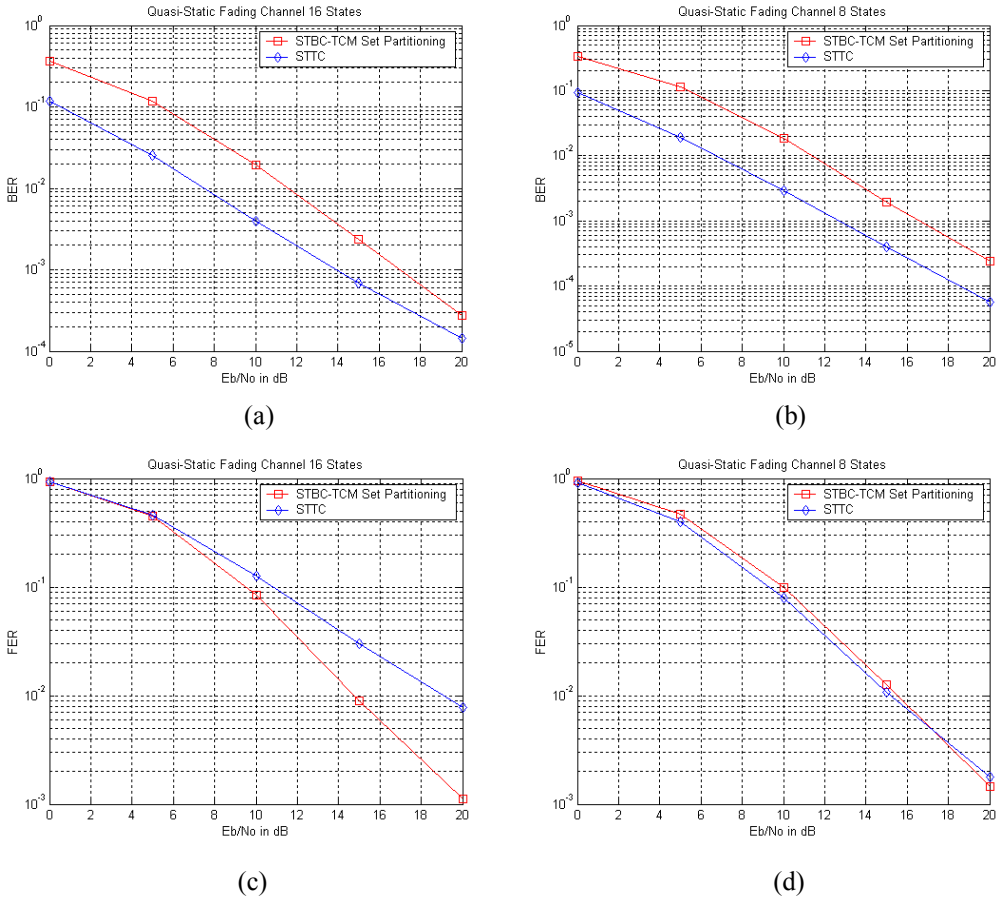

Figure 2.9 STTC compared with STBC-TCM for the quasi-static fading channel. (a) BER 16 State (b) BER 8 State (c) FER 16 State (d) FER 8 State.

2.6 Chapter Summary

In this chapter discussed, three space-time coding techniques; Space Time Trellis Coding, Space Time Block Coding, and a concatenated Space Time Block Coding-Trellis Coded Modulation. Different mapping techniques were examined for the STBC-TCM under both channel scenarios. For the quasi-static channel, Gray coding provides the best BER performance. However, for the block fading channel, set-partitioning provides the best BER performance. It was shown that for the quasi-static channel, adding TCM to the STBC does not improve the BER performance. When the channel is constant over the

length of each codeword, there is not enough diversity present to allow for any significant coding gain.

The structure of the concatenated STBC-TCM system is very similar to STTC. For systems with the same spectral efficiency and trellis complexity, STTC provides the best BER performance for the quasi-static fading channel. STBC-TCM provides the best BER performance for block fading channel. Ultimately, the choice between STBC-TCM and STTC depends on what is more important, frame error rate or bit error rate.

Chapter 3

Vertical Bell-Labs Layered Space Time (V-BLAST) Architecture

3.1 Introduction

Vertical **B**ell-Labs **L**ayered **S**pace **T**ime (V-BLAST) architecture was first proposed by Foschini to increase capacity while exploiting multipath fading [4]. Multiple transmit antennas are used to simultaneously transmit independent data; this results in an increase in the data rate proportional to the number of transmit antennas. Each transmitter uses the same frequency spectrum for every transmission which leads to high spectral efficiency.

V-BLAST is a single user system where the basic detection algorithm is based on the concept of multi-user detection. The suboptimum algorithm sequentially detects the symbols through ordering, linear nulling, and symbol cancellation. Perfect channel knowledge is assumed to be available at the receiver. Either Zero Forcing and Minimum Mean Squared Error criteria can be used for nulling. The performance is limited by error propagation and imperfect channel estimation.

This chapter covers the basic principles and detection algorithm for V-BLAST. In addition, the error propagation problem that results from the successive interference cancellation is examined. Finally, the perfect channel knowledge assumption is removed and Least Squares and MAP Estimation are used to investigate the performance in the

presence of unknown channel characteristics. Simulation results are provided throughout the chapter.

3.2 V-BLAST Architecture

Figure 3.1 shows a block diagram of the V-BLAST architecture. There are N_t transmit antennas and N_r receive antennas, where $N_r \geq N_t$. The data is first demultiplexed into layers, or parallel sub-streams, and each layer is transmitted from a different antenna. Each antenna transmits the data layers simultaneously in the same frequency band. The channel is assumed to be quasi-static, flat, Rayleigh fading. The receivers operate co-channel where the signal at each receiver contains superimposed components of the transmitted signals.

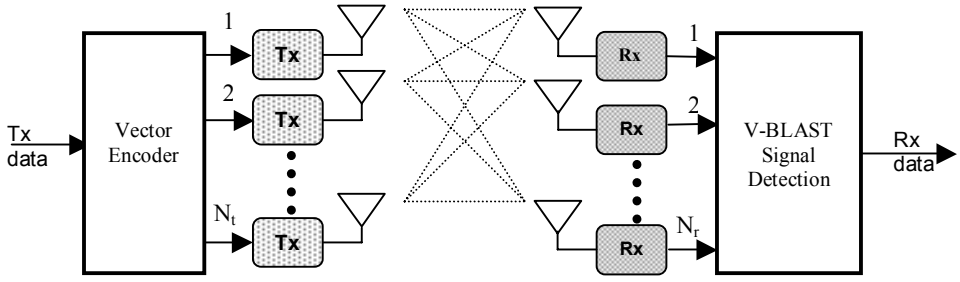

Figure 3.1 Block diagram of V-BLAST architecture

The V-BLAST system model can be represented in matrix notation. The vector of transmitted symbols, at time k, is represented by

$$x_k = [x_k(1) \quad x_k(2) \quad \cdots \quad x_k(N_t)]^T \tag{3.1}$$

Each receive antenna receives signals from all N_t transmit antennas. The received signal during the kth time interval is expressed as

$$r_k = \mathbf{H}x_k + v_k \tag{3.2}$$

where **H** is the channel matrix given by (1.1), and v_k is the noise vector given by

$$v_k = [v_k(1) \quad v_k(2) \quad \cdots \quad v_k(N_r)]^T \tag{3.3}$$

where v is assumed to be i.i.d. additive white Gaussian noise with zero mean and co-variance matrix $I\sigma_n^2$.

The V-BLAST detection algorithm utilizes interference suppression and symbol cancellation to successively detect symbols from each transmit antenna. When detecting the i^{th} symbol, all other symbols are treated as interferers. Linear nulling is used in interference suppression by weighting the received vector to satisfy a performance criterion, such as zero-forcing or minimum mean squared error (MMSE). The nulling matrix for zero forcing (ZF) is given by:

$$G = (H^H H)^{-1} H^H \tag{3.4}$$

while the nulling matrix for the minimum mean squared error (MMSE) criteria is given by:

$$G = (H^H H + \frac{\sigma_n^2}{\sigma_d^2} I)^{-1} H^H \tag{3.5}$$

where σ_d^2 / σ_n^2 is the signal to noise ratio.

The i^{th} nulling vector nulls all but the i^{th} transmitted signal from the received signal, given by

$$w_i = (G)_i^H$$

where $(G)_i$ is the i^{th} column of the nulling matrix G, and $(\cdot)^H$ is the conjugate transpose.

The nulling vector multiplied by the received signal vector suppresses all layers except the i^{th} layer. A decision statistic, y_i, is calculated from the nulling vector, $y_i = w_i^T r$. The maximum likelihood estimate, $\tilde{x}_i$, is determined from y_i. The estimated symbol is

assumed to be correct and used for symbol cancellation. Interference from the already detected components of x are subtracted from the received signal vector. The updated received symbol is given by

$$r = r - \tilde{x}_i (H)_i \tag{3.6}$$

The optimal detection order detects the symbols in order of decreasing signal strength. The strongest layer has the largest post detection signal to noise ratio, given by

$$\rho_{ki} = \frac{E\{|\, x_{ki}\,|^2\}}{\sigma^2 \,||\, w_{ki}\,||^2} \tag{3.7}$$

The layer with the largest post detection signal to noise ratio corresponds to the nulling vector with the minimum norm squared.

The column of **H** that corresponds to the symbol most recently detected is removed and the nulling matrix is recalculated. The detection process is repeated until all transmitted symbols are detected.

Figure 3.2 compares the bit error rate (BER) versus signal to noise ratio for different versions of the V-BLAST algorithm. These plots show the average BER for all transmitted layers. The Ordered MMSE algorithm yields the best BER performance, whereas the unordered ZF algorithm yields the worst. The Ordered Algorithm detects the strongest signal first. As a result, the strongest interference is cancelled first. On average, this leads to improved BER performance in the sequentially detected layers. The MMSE nulling criteria utilizes knowledge of the signal to noise ratio to improve performance.

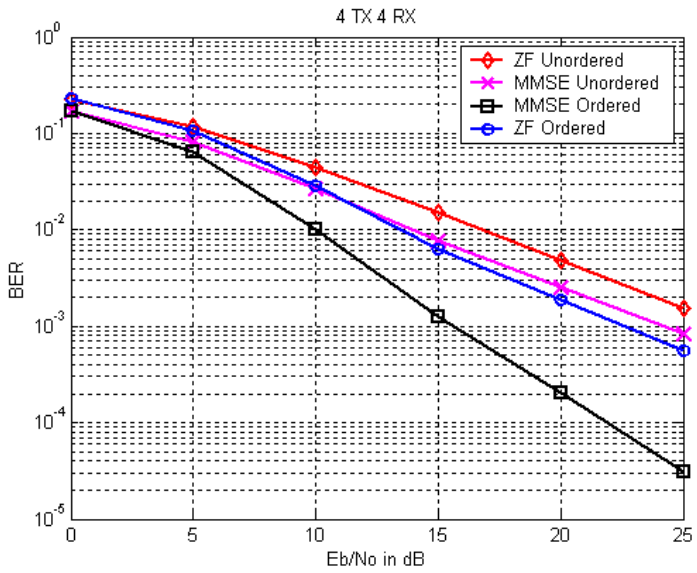

Figure 3.2 Different V-BLAST Algorithms

Figure 3.3 shows the diversity gain that results from increasing the number of receive antennas. The increase in slope of the bit-error-rate curve corresponds to a diversity gain in the system.

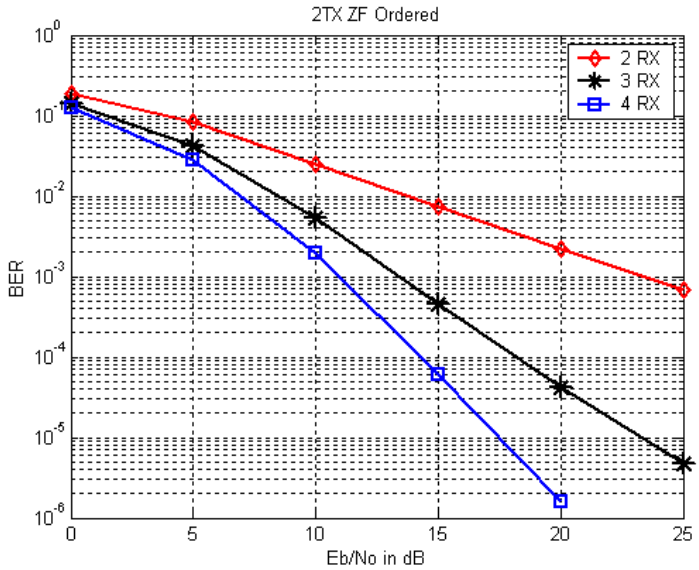

Figure 3.3 Two Transmit Antennas and varying number of Receive Antennas

3.3 Error Propagation

After each symbol is cancelled from the received vector, the number of symbols remaining to be detected is reduced, while the number of receive antennas remains the same. Theoretically, since less nulling is required, the diversity level should increase from layer to layer. During the symbol cancellation step, all previous decisions are assumed to be correct. When an incorrect decision is made, interference can be added in, rather than being subtracted out. This may result in errors propagating into the subsequent layers. The received signal after detecting (k-1) layers is given by [19]

$$r_{i+k} = H_k x_k(i) + \sum_{j=1}^{k-1} H_j \left(x_j(i) - \tilde{x}_j(i) \right) + \sum_{j=k+1}^{N_t} H_j x_j(i) + v(i) \tag{3.8}$$

where r_k is the received signal after cancellation of all but the k^{th} layer, H_k is the k^{th} column of the channel matrix, and $\tilde{x}_k$ is the decoded symbols in the k^{th} step

The first term in equation 3.8 is the desired layer, the second term is the interference from previously cancelled layers, the third term is the interference due to the uncancelled layers, and the forth term is additive white Gaussian noise. The second term is equal to zero when a symbol is detected correctly, that is when $x_j(i) = \tilde{x}_j(i)$.

Additional layers provide the receiver information that can help to properly decode the transmitted symbols. However, when the symbols are detected incorrectly, the additional layers actually add more interference to the system. As a result, the additional layers do not generally improve system performance.

Figure 3.4 shows the difference between ideal cancellation and actual cancellation for the individual layers of the zero forcing unordered algorithm with four transmit and four receive antennas. In ideal cancellation, known transmitted symbols are used for the

interference cancellation, whereas in the actual cancellation the detected symbols are used for interference cancellation. There is no performance improvement for the first layer detected with ideal cancellation compared to actual cancellation. However, for ideal cancellation, each layer benefits from subtraction of the previously detected symbols, resulting in a diversity gain from layer to layer. The increasing slope of the BER curve of the ideal cancellation represents the diversity gain.

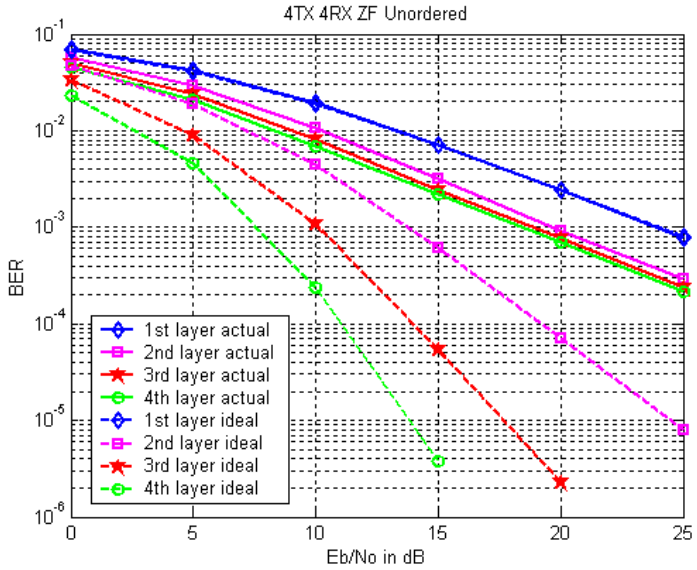

Figure 3.4 Effect of Error Propagation

3.4 Channel Estimation

The assumptions of the V-BLAST algorithm depend on perfect channel knowledge at the receiver. However, in a real system, perfect channel knowledge is not attainable. The channel is often estimated using pilot symbols.

Figure 3.5 shows the BER when the estimated channel is modeled as the true channel plus AWGN. Constant channel estimation errors yield error floors at high signal to noise ratio. At low SNR, errors are dominated by noise, whereas at high SNR errors are dominated by channel estimation errors.

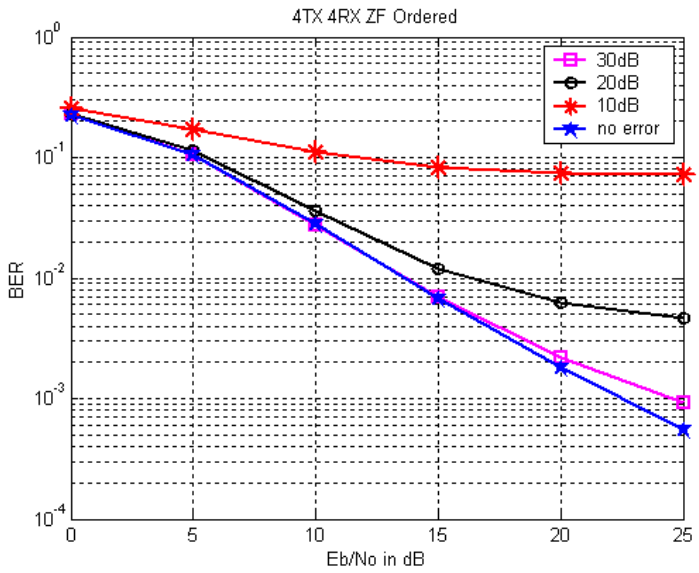

Figure 3.5 V-BLAST with Constant Channel Estimation Errors

3.4.1 Least Squares Channel Estimation

Least squares (LS) estimation requires pilot symbols and matrix inversion. A training sequence (known to the receiver) is transmitted by each transmit antenna at the beginning of each data burst. The training sequence consists of pilot symbols that are orthogonal across the different transmit antennas. The *L x 1* training sequence for the j[th] transmit antenna is given by

$$x_j = \left[x_j(0) \quad x_j(1) \quad \cdots \quad x_j(L-1)\right]^T \tag{3.9}$$

The $L \times N_t$ orthogonal training sequence matrix for all N_t transmit antennas is given by

$$\mathbf{X} = \left[x_1; \quad x_2; \quad \cdots; \quad x_{N_t}\right] \tag{3.10}$$

where $x_i^T x_j^T = \begin{cases} L & i = j \\ 0 & i \neq j \end{cases}$

The received signal matrix during the training period is given by

$$\mathbf{R} = \mathbf{HX} + V \tag{3.11}$$

where **H** is the channel matrix, **X** is the training sequence matrix, and V is the noise vector.

The ML estimate for the channel matrix is given by [20]

$$\begin{aligned}\hat{\mathbf{H}} &= \mathbf{R}\mathbf{X}^{\dagger} \\ \hat{\mathbf{H}} &= (\mathbf{H}\mathbf{X} + \mathbf{V}) \cdot \mathbf{X}^{\dagger} \\ \hat{\mathbf{H}} &= \mathbf{H} + \mathbf{V}\mathbf{X}^{\dagger}\end{aligned} \tag{3.12}$$

where $\mathbf{X}^{\dagger} = (X^H X)^{-1} X^H$ is the Moore-Penrose Pseudoinverse.

The estimation error is given by

$$\Delta\mathbf{H} = \mathbf{V}\mathbf{X}^{\dagger} \tag{3.13}$$

The computational complexity of LS estimation depends on the number of transmit antennas and the number of training symbols per antenna. To achieve the same BER performance, more pilot symbols are required as the number of transmit antennas increases. A longer training sequence matrix results in a more complex matrix inversion. The computational complexity of finding the pseudoinverse of a L x N_t training sequence matrix is $O(L^2 N_t + L N_t^2 + \min(L, N_t)^3)$ [21]. For example, doubling the number of training symbols per transmit antenna from eight to sixteen, assuming four transmit antennas, results in a increase in complexity on the order of 200%.

3.4.2 MAP Channel Estimation

Maximum *a posteriori* (MAP) channel estimation is an alternative to Least Squares estimation that yields comparable performance in the Rayleigh fading channel. MAP channel estimation requires knowledge of the training sequence, the channel covariance, and the noise covariance at the receiver. The same system model described for LS estimation applies to MAP estimation.

The MAP estimate for the channel matrix maximizes the a posteriori probability density function p(H|r,X) with respect to **H** [22]. The map estimate for **H** satisfies

$$\frac{\partial}{\partial H} \ln p(H \mid r, X)\Big|_{H=\hat{H}_{map}(X)} = 0 \tag{3.14}$$

Baye's rule states that

$$p(H \mid r, X) = \frac{p(r \mid H, X)p(H \mid X)}{p(r \mid X)} \tag{3.15}$$

where

$$p(r \mid H, X) = \pi^{-L}\left|R_n\right|^{-1} \exp(-(r - XH)^H R_n^{-1}(r - XH)) \tag{3.16}$$

and

$$p(H \mid X) = \pi^{-NL}\left|R_H\right|^{-1} \exp(-H^H R_H^{-1} H) \tag{3.17}$$

R_n is the noise covariance and R_h is the channel covariance. For independent Rayleigh fading channels, R_h can be approximated as an identity matrix.

Solving (3.14) yields the MAP estimate

$$\hat{H}_{map}(X) = \left(X^H R_n^{-1} X + R_H^{-1}\right)^{-1} X^H R_n^{-1} r \tag{3.18}$$

An N_t x N_t matrix inversion is required to find the MAP estimate. The computational complexity for the matrix inversion remains constant as the number of training symbols increases. However, the total computational complexity of the MAP estimate requires $2L^2N_t + LN_t^2 + LN_tN_r + N_t^2N_r$ multiplications, $2L^2N_t + N_t^2(L+1) + LN_tN_r + N_t^2N_r$ additions, and $O(N_t^3)$ operations for the matrix inversion. Even though the size of the matrix to be inverted depends only on the number of transmit antennas, the complexity still depends on the number of training symbols.

Figure 3.6 shows simulation results for LS and MAP estimation with four transmit and receive antennas and two transmit and receive antennas. Almost identical BER performance results from MAP and LS channel estimation. Surprisingly, knowledge of channel statistics, required for MAP estimation, did not yield better channel estimates than LS estimation. For four transmit antennas, approximately sixteen training symbols per transmit antenna (64 training symbols total) are required to be within approximately 1 dB of the perfectly known channel. For two transmit antennas, approximately eight training symbols per transmit antenna (16 training symbols total) are required to be within approximately 1 dB of the perfectly known channel.

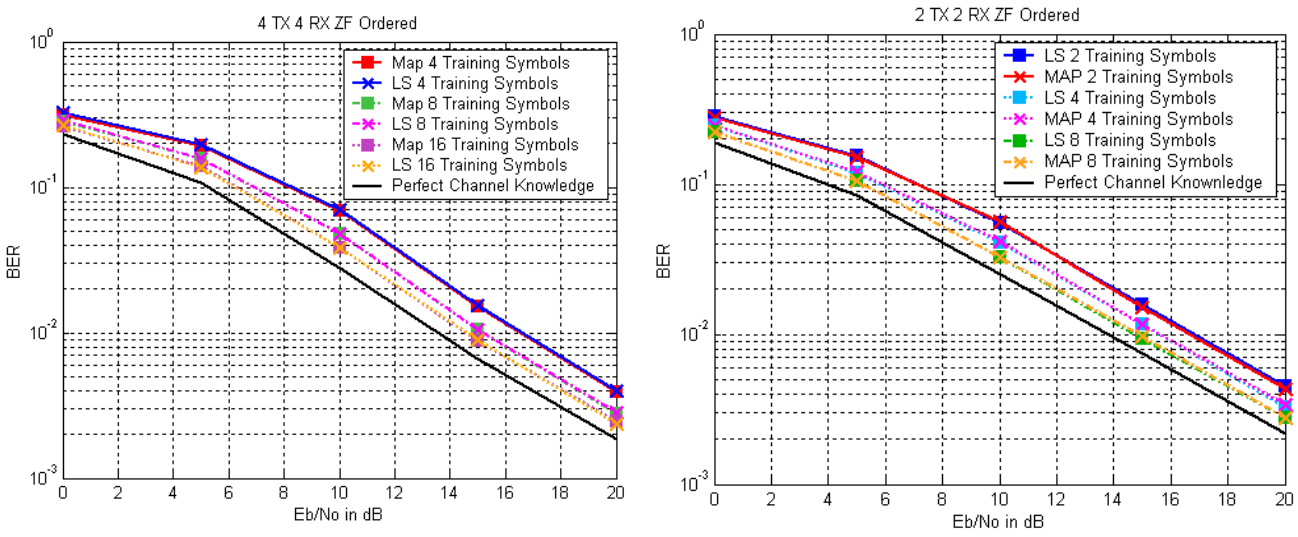

Figure 3.6 LS and MAP Estimation (a) Four Transmit and Four Receive Antennas. (b) Two Transmit and Two Receive Antennas

3.5 Chapter Summary

In this chapter, the V-BLAST architecture and detection procedure was introduced. Simulations showed that the ordered algorithm with MMSE criteria yielded the best bit error rate performance. Error propagation was shown to limit the theoretical performance

of V-BLAST. Finally, the performance with imperfect channel knowledge was examined. The performance of V-BLAST using Least Squares Estimation and MAP Estimation were shown to approach the perfect channel knowledge case at the cost of increased complexity. The computation complexity of LS estimation increases exponentially as the number of training symbols increases, whereas MAP estimation requires knowledge of the channel statistics in addition to increased complexity compared with LS. Furthermore, MAP estimation provides no performance improvement when compared with LS estimation. The results presented in this chapter emulate those already published in the literature.

Chapter 4

Coded V-BLAST Systems

4.1 Introduction

The simple encoding procedure of the V-BLAST architecture paves the way for concatenation with convolutional coding. The overall system performance should improve after the addition of convolutional coding. However, it will be shown that under certain channel conditions, combining convolutional coding with V-BLAST actually hinders the BER performance. Combining convolutional coding with an iterative V-BLAST algorithm performs better than the original coded V-BLAST algorithm, when performed under identical channel conditions. The iterative V-BLAST algorithm was originally proposed to alleviate the error propagation effects present in the original V-BLAST algorithm [8]. Finally, a coded V-BLAST-OFDM system is described for frequency selective fading channels.

This chapter is organized as follows. Chapter 4.1 discusses the original V-BLAST algorithm combined with convolutional coding. Chapter 4.2 summarizes an iterative V-BLAST detection algorithm. Chapter 4.3 discusses the iterative V-BLAST algorithm combined with convolutional coding. Chapter 4.4 considers coded V-BLAST-OFDM systems for the frequency selective quasi-static channel. Simulation results and analysis are provided throughout the chapter.

4.2 Coded Original V-BLAST

Addition of error correction coding to the V-BLAST architecture should enhance BER performance by providing coding gain. Figure 4.1 shows the block diagram for the transmitter of a coded V-BLAST system. The channel codes considered are convolutional codes with varying constraint lengths. The data and pilot symbols are encoded by the channel encoder, passed through an interleaver, and then demultiplexed and distributed to the transmit antennas. The pilot symbols are sent through the channel encoder to jump start the decoding process at the receiver.

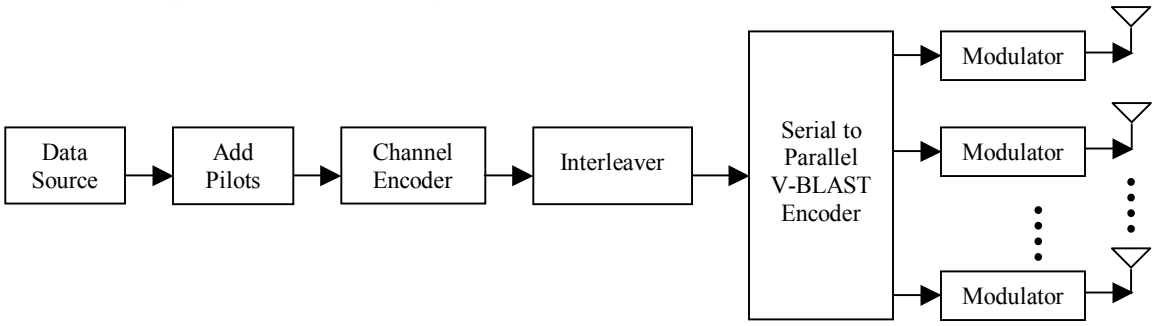

Figure 4.1 Coded V-BLAST Transmitter Block Diagram

The encoded data from a single convolutional code is divided amongst all transmit antennas. Alternatively, each layer could be coded individually (after the V-BLAST encoder). A third option would be to apply coding before and after the V-BLAST encoding [23]. Both alternatives cause significant increase in complexity, since they require multiple decoders at the receiver. Therefore, consideration is given only to systems where the coding is applied before the V-BLAST encoding.

Figure 4.2 shows a block diagram of the receiver in a coded V-BLAST system. The channel is estimated at the receiver. The estimated channel information and received signals are sent to the V-BLAST decoder. The output of the V-BLAST decoder is converted from parallel to serial and then deinterleaved. The channel decoders

considered are the hard decision Viterbi algorithm and the hard decision BCJR algorithm [24].

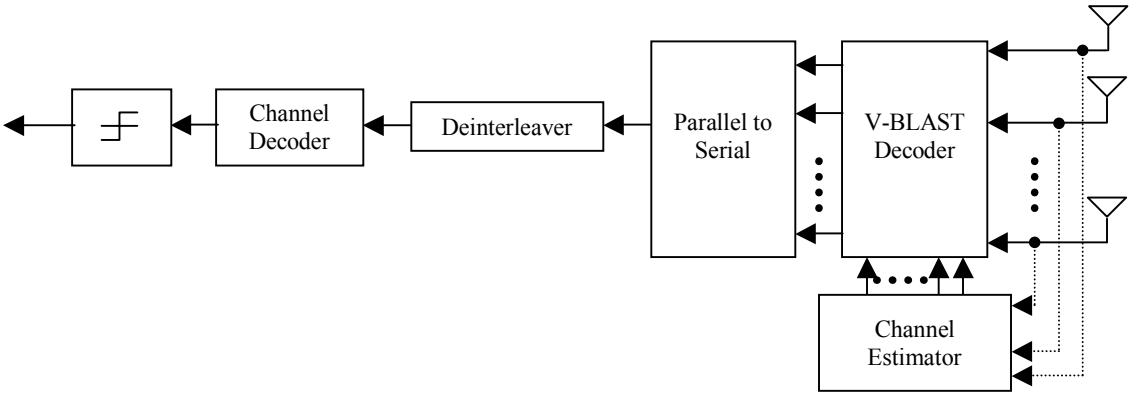

Figure 4.2 Coded V-BLAST Receiver Block Diagram

Figure 4.3 shows simulation results of a coded V-BLAST system consisting of four transmit antennas, four receive antennas and the zero forcing ordered detection algorithm. The implemented convolutional codes include the rate ½ constraint length seven code (generator polynomials $(133,171)_{octal}$) and the rate ½ constraint length three code (generator polynomials $(5,7)_{octal}$). The channel decoder uses hard decisions from the V-BLAST decoder. The quasi-static channel is constant over a frame of length 200 symbols. When compared with the uncoded V-BLAST system, the coded system actually performs worse. The lack of performance improvement may result from making hard decisions on the decoded symbols. Additionally, the performance may be limited by burst errors resulting from the error propagation problem. The constraint length three code outperforms the constraint length seven code. The more powerful codes break down faster in a diversity-limited environment. The BER performance of the coded V-BLAST system in a quasi-static environment is limited by the performance of the convolutional codes in the same environment. There is not enough diversity present in

the quasi-static environment for the channel decoder to be able to properly distinguish between symbols.

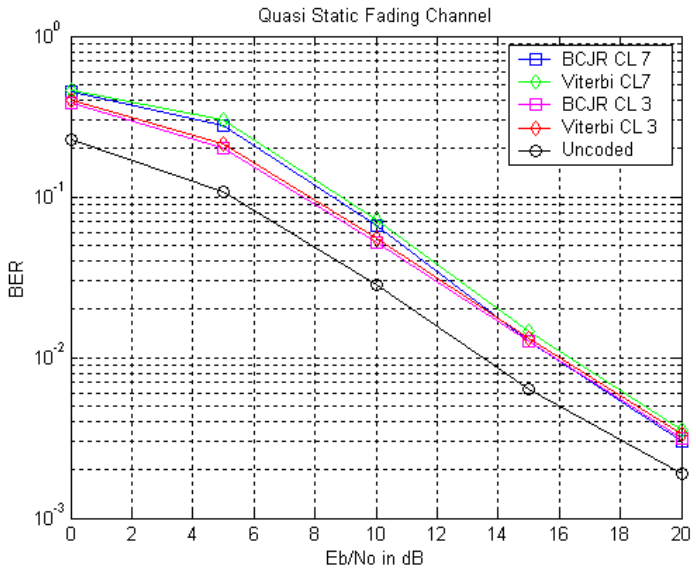

Figure 4.3 Coded System with the Quasi-Static Channel Model

The above simulations were repeated using the block fading channel model. Figure 4.4 shows that there for the constraint length seven code there is significant gain over the uncoded V-BLAST system (approximately 8 dB at 10^{-3}). For both channel models, the increased complexity of the BCJR algorithm provides no additional gain over the Viterbi algorithm.

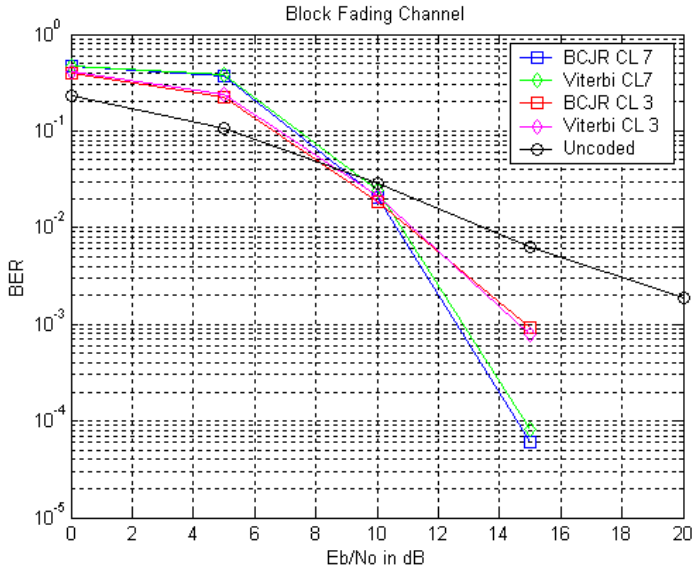

Figure 4.4 Coded system with the Block Fading Channel Model

4.3 Iterative V-BLAST Algorithm

Many different detection algorithms have been proposed for the V-BLAST architecture. An iterative soft interference cancellation algorithm was proposed to alleviate error propagation effects present in the original V-BLAST detection algorithm [8]. When combined with convolutional coding, this algorithm outperforms the uncoded system for the quasi-static channel. The proposed algorithm uses MAP criteria and limits the increase in computational complexity. Interference from the more certain symbols is subtracted from the less certain symbols. The symbols are iteratively updated using the *a posteriori* probability.

The algorithm first determines initial soft symbol estimates (χ's) according to

$$z = H^H (HH^H)^{-1} r \tag{4.1}$$

The real and imaginary part of χ_k are scaled according to

$$\mathrm{Re}(\chi_k)=\begin{cases} x_{\min} & \text{if } \mathrm{Re}(z_k) < x_{\min} \\ \mathrm{Re}(z_k) & \text{if } x_{\min} \le \mathrm{Re}(z_k) \le x_{\max} \\ x_{\max} & \text{if } \mathrm{Re}(z_k) > x_{\max} \end{cases} \quad \mathrm{Im}(\chi_k)=\begin{cases} x_{\min} & \text{if } \mathrm{Im}(z_k) < x_{\min} \\ \mathrm{Im}(z_k) & \text{if } x_{\min} \le \mathrm{Im}(z_k) \le x_{\max} \\ x_{\max} & \text{if } \mathrm{Im}(z_k) > x_{\max} \end{cases}$$

where x_{min} is -1 and x_{max} is +1 for QPSK.

Next, the soft symbol estimates are cancelled from the received signal vector

$$z_{i,k} = r_i - \sum_{j \neq k} h_{i,j} \chi_k \tag{4.2}$$

In each iteration, the soft symbols estimates for the k transmitted symbols are iteratively updated from

$$\chi_k = \frac{\sum_{i=1}^{4} \alpha_i \; p(r \mid x_k = \alpha_i)}{\sum_{i=1}^{4} p(r \mid x_k = \alpha_i)} \tag{4.3}$$

where α_i is one of the four QPSK symbols, and the a posteriori probability is given by

$$p(r \mid x_k = \alpha) = \prod_i \frac{1}{\pi \sigma_{i,k}^2} \exp\left(\frac{-\left| z_{i,k} - h_{i,k} \alpha \right|^2}{\sigma_{i,k}^2} \right) \tag{4.4}$$

and $\sigma_{i,k}^2$ is the total interference plus noise power between transmit antenna k and receive antenna i, given by

$$\sigma_{i,k}^2 = \sigma_n^2 + \sum_{j \neq k} \left| h_{i,j} \right|^2 e_j^2 \tag{4.5}$$

where σ_n^2 is the noise power, and e_j^2 is the variance of the jth transmitted symbol. The variance about each soft symbol quantifies the reliability of each soft symbol. The variance is given by

$$e_k^2 = \frac{\sum_{i=1}^{4} |\alpha_i - \chi_k|^2 \, p(r \mid x_k = \alpha_i)}{\sum_{i=1}^{4} p(r \mid x_k = \alpha_i)} \tag{4.6}$$

Examination of BER performance per layer provides insight into the error propagation effect. Figure 4.5 shows that all layers yield approximately the same BER performance; indicating no significant error propagation. The lack of ordering in the iterative V-BLAST algorithm helps alleviate the error propagation present in the original V-BLAST algorithm.

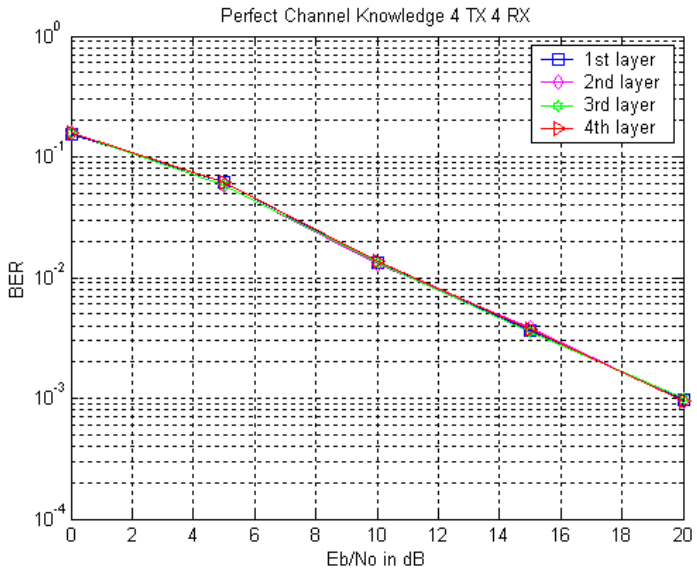

Figure 4.5 Error Propagation in Iterative Soft Interference Cancellation Algorithm

Figure 4.6 shows the convergence rate of the iterative soft interference cancellation algorithm. After approximately three iterations, the performance increase is insignificant, and the algorithm has converged.

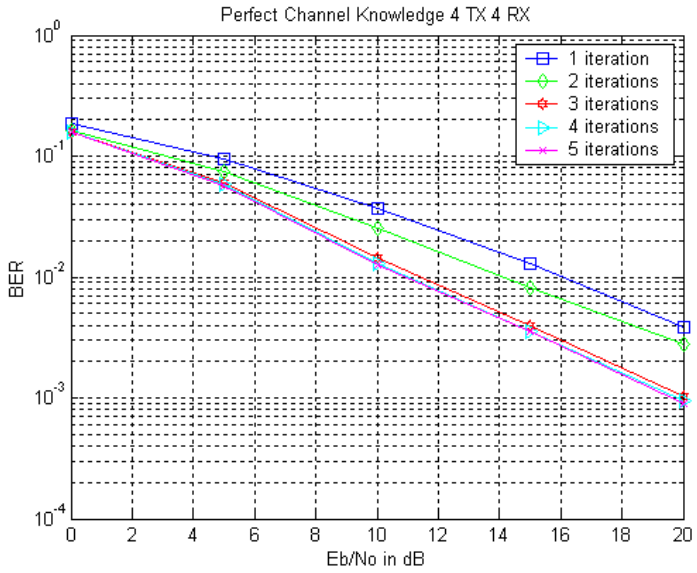

Figure 4.6 Convergence Rate of the Iterative Soft Interference Cancellation Algorithm

Figure 4.7 shows a comparison between the iterative algorithm and the original V-BLAST algorithm. The iterative algorithm outperforms the original algorithm by approximately 3 dB. The reduced error propagation effect (from the lack of ordering) leads to the performance improvement in the iterative V-BLAST algorithm.

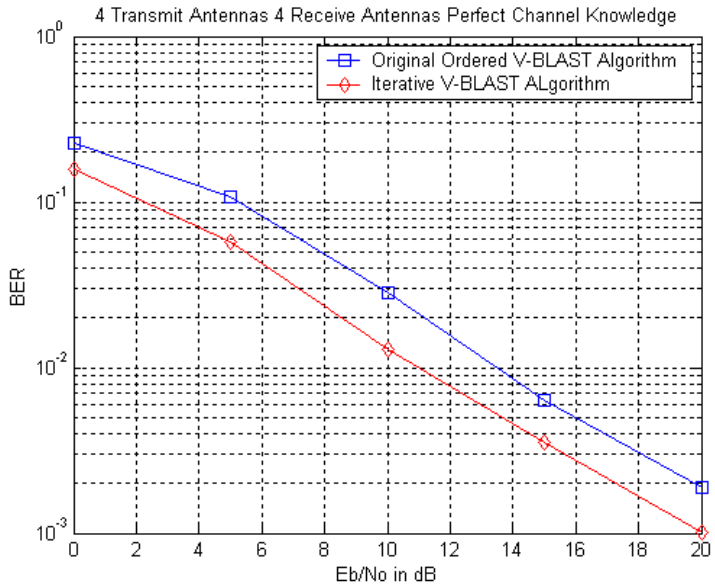

Figure 4.7 Comparison between original and iterative V-BLAST algorithms

4.4 Coded Iterative V-BLAST Algorithm

Convolutional coding can be combined with the iterative V-BLAST algorithm, as with the original V-BLAST algorithm. The same system as the original coded V-BLAST system is considered; constraint length seven and constraint length three convolutional codes for the quasi-static and block fading channel models. In addition to hard decision decoding, the channel decoders under consideration include soft decision decoding with the Viterbi and BCJR algorithms. The branch metrics for soft decision decoding are calculated from the final estimates for all χ_k's (equation 4.3). Another approach considers the final probability information determined from the iterative V-BLAST (equation 4.4) algorithm as *a priori* probability information in the BCJR algorithm. This can be applied with both hard and soft decision decoding.

Figure 4.8 shows the performance of the coded iterative V-BLAST system for the quasi-static channel. Figure 4.8 (a) shows the constraint length seven code, while figure 4.9 (b) shows the constraint length three code. Six different decoding strategies are considered; hard decision Viterbi decoding, hard decision BCJR decoding, soft decision Viterbi decoding, soft decision BCJR decoding, soft decision BCJR decoding with *a priori* probability information, and hard decision BCJR decoding with *a priori* probability information. Soft decision decoding outperforms hard decision decoding by approximately 1 ½ dB at 10^{-2} for the constraint length seven code. For both codes, combining the *a priori* probability information with soft decision decoding performs the best. The constraint length seven code provides approximately 1 dB of coding gain over hard decision decoding, and 3 dB over soft decision decoding. The coded system outperforms the uncoded system by approximately 6 dB at 10^{-3}. For the constraint length

three code, soft decision decoding with the a priori probability information outperforms the uncoded system by only 1 dB at 10-3. Hard decision decoding does not outperform the uncoded system for the constraint length three code. Combining the *a priori* probability information with hard decision decoding outperforms soft decision decoding. The *a priori* probability information provides more distinguishing information to the BCJR decoder than the soft decision information.

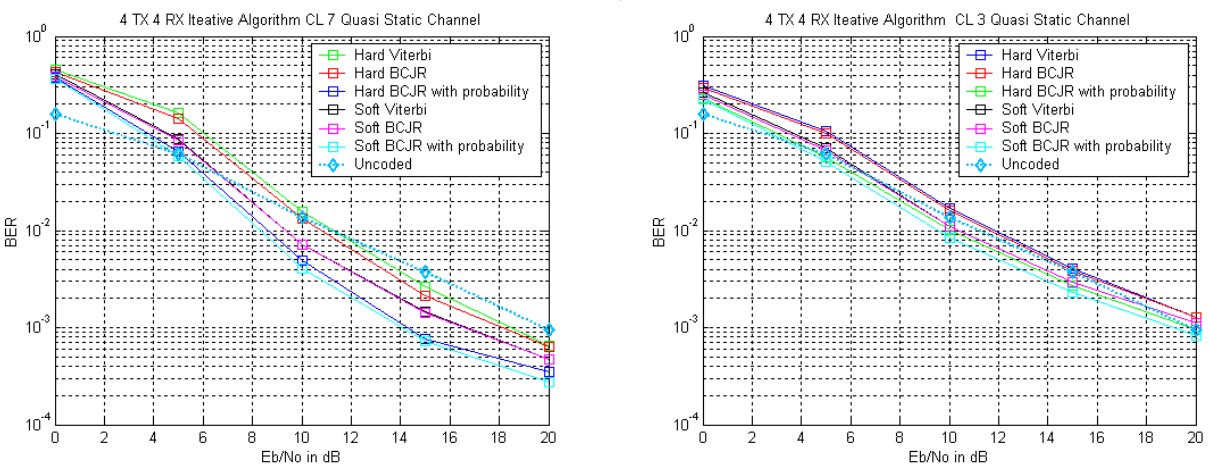

(a) (b)

Figure 4.8 Coded System for the Quasi-Static Channel. (a) Constraint length 7 code. (b) Constraint length 3 code.

For the block fading channel, figure 4.9 (a) shows simulation results for the constraint length seven code, and figure 4.9 (b) shows the constraint length three code. The same six decoding strategies were tested. As with to the quasi-static channel case, the use of *a priori* probability information, with soft decision BCJR decoding, yields the most coding gain. The coded system outperforms the uncoded system by 10 dB for the constraint length seven code, and 2 dB for the constraint length three code at 10^{-3}. Additionally, for both channel models, the BCJR algorithm without the a priori probability information provides no significant improvement over the Viterbi algorithm.

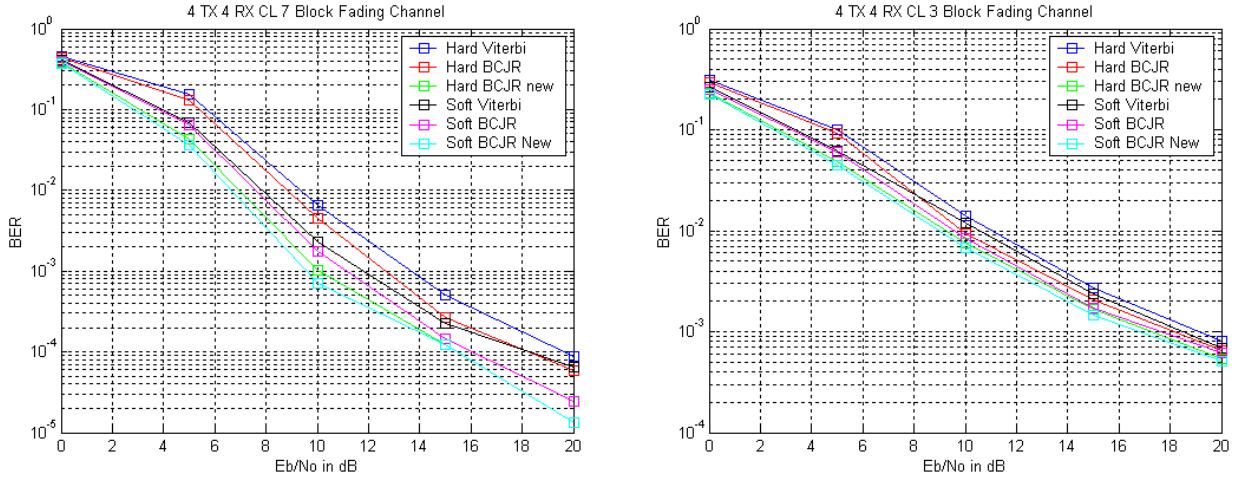

Figure 4.9 Coded System for the block fading channel. (a) Constraint length 7 code. (b) Constraint length 3 code.

Under the quasi-static channel assumption, the coded iterative V-BLAST algorithm outperforms the uncoded iterative V-BLAST; whereas the coded original V-BLAST performance is hindered by the addition of coding. Even with hard decision decoding, the addition of coding to the iterative V-BLAST algorithm results in a slight coding gain. However, the coding gain obtained under quasi-static channel conditions falls short of the coding gain obtained the block fading channel by 4 dB. Since both hard and soft decision decoding outperform the uncoded case, the robustness of the iterative V-BLAST algorithm is the main reason for improvement. The reduced error propagation effects in the iterative V-BLAST algorithm is a likely contributor to the coding gain obtained using the iterative V-BLAST algorithm in the quasi-static channel.

4.5 Coded V-BLAST-OFDM Systems

Frequency-selective fading can severely impair the performance of coded V-BLAST systems [25]. Orthogonal frequency division multiplexing (OFDM) has emerged as a

dominant solution to combat frequency-selective multipath fading [25]. OFDM is a multi-carrier modulation technique where data is transmitted simultaneously over different subcarriers. OFDM systems divide frequency selective channels into multiple subchannels, where each subchannel exhibits flat fading characteristics. Each transmitted symbol occupies a small fraction of the available bandwidth. The orthogonal and overlapping frequency response of the subcarriers leads to increased spectral efficiency.

The inverse discrete Fourier transform (IDFT) generates the OFDM symbols. A cyclic prefix (CP) is appended to the front of each OFDM symbol. Cyclic prefixes create a guard band around individual OFDM symbols, thereby reducing inter-symbol interference [25]. The cyclic prefix is a copy of the last part of the OFDM symbol. The OFDM symbol length is greater than or equal to the length of the largest delay spread of the channel.

The combination of OFDM and V-BLAST can overcome intersymbol interference in frequency selective fading channels [26]. Figure 4.10 shows a block diagram of a V-BLAST-OFDM transmitter. A vector symbol of size N_t is transmitted across every subchannel at every time interval. After channel encoding, the desired data is first demultiplexed into N_t parallel sequences. A serial to parallel converter converts each N_t sequence into L subsequences; one for each subcarrier. Finally, the data passes through an IFFT block, the cyclic prefix is appended, and the OFDM symbols are transmitted over each transmit antenna.

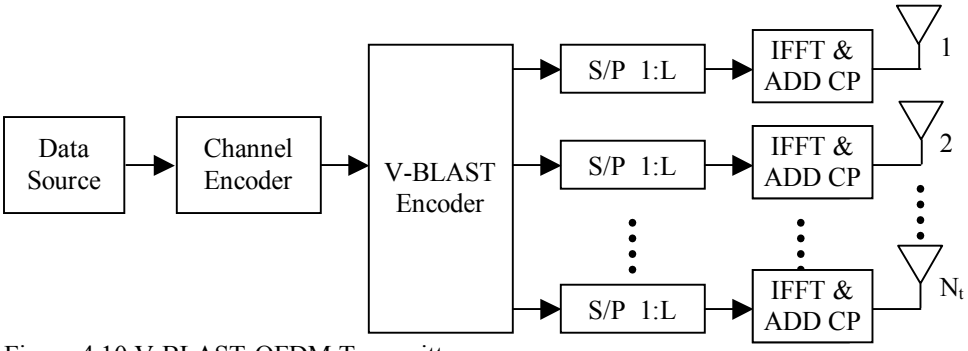

Figure 4.10 V-BLAST-OFDM Transmitter

Figure 4.11 shows the block diagram of a V-BLAST-OFDM receiver. Each receive antenna receives a signal for each of the L subchannels. After the cyclic prefix is removed, each received signal passes through a FFT block for demodulation.

The received signal after demodulation, at receive antenna *m* for subchannel *l*, is given by

$$r_{m,l} = \sum_{n=1}^{N_t} h_{m,n,l} C_{n,l} + v_{m,l} \quad l = 1,\ldots L \tag{4.7}$$

where $h_{m,n,l}$ is the channel path from transmit antenna *n* to receive antenna *m* at frequency *l*, $C_{n,l}$ is the OFDM symbol transmitted from antenna *n* at frequency *l*, and $v_{m,l}$ are independent Gaussian noise samples. The outputs of the FFT blocks are passed to *L* V-BLAST detectors, each with N_r inputs, and N_t outputs. The outputs of the V-BLAST detectors are converted from parallel substreams to serial data stream. Finally, the data is decoded by the channel decoder.

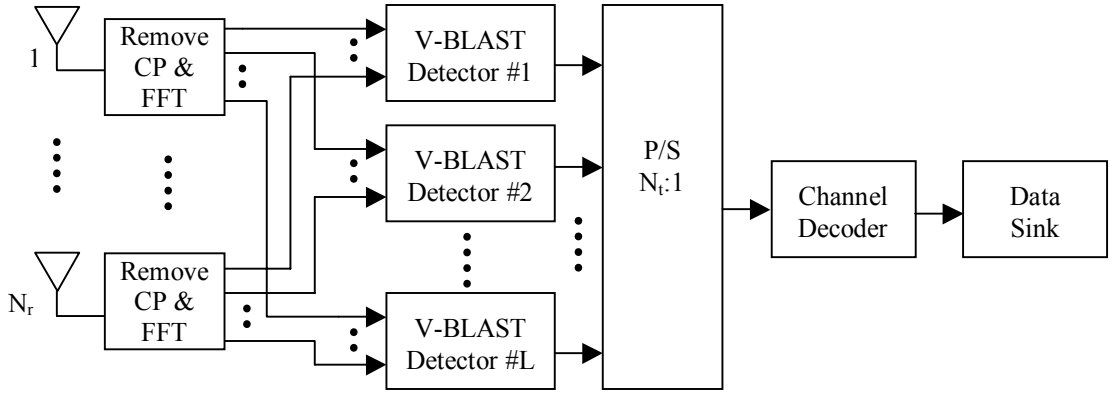

Figure 4.11 V-BLAST-OFDM Receiver

For the quasi-static frequency selective fading channel, coded V-BLAST-OFDM systems can achieve performance equivalent to the coded V-BLAST system for the frequency non-selective fading channel. For a large number of subcarriers, OFDM divides the frequency-selective channel into completely independent Rayleigh flat fading channels. Increasing the number of subcarriers is equivalent to increasing the interleaver depth in a frequency non-selective channel. Using OFDM for the frequency non-selective fading channel does not yield any change in performance. For the frequency non-selective channel, dividing the channel into subchannels does not introduce any new channel paths. The performance of the above described coded V-BLAST-OFDM system was examined for both the original and iterative V-BLAST detection algorithms. The soft decision BCJR algorithm, without *a priori* probability information, is the channel decoder considered for the coded iterative V-BLAST system. The hard decision BCJR algorithm is the channel decoder considered for the coded original V-BLAST system. The implemented channel code is the constraint length seven convolutional code. In the following simulations, the amount delay spread present in the frequency selective fading channel is varied. The number of subcarriers is the minimum number of subcarriers required to overcome the amount of delay spread that is present. For example, only eight subcarriers may be required to overcome a small delay spread.

Figure 4.12 shows the performance of the coded original V-BLAST-OFDM system. The number of subcarriers varies between one and two-hundred and fifty-six.

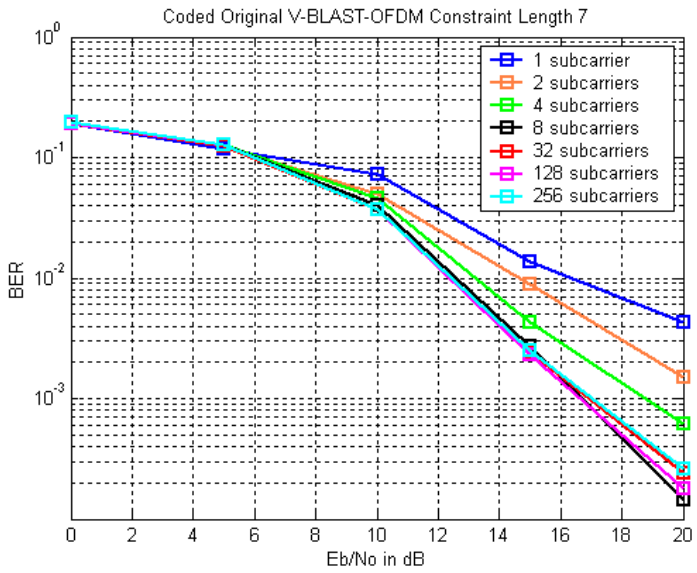

Figure 4.12 Coded Original V-BLAST-OFDM System

Figure 4.13 shows the performance of the coded iterative V-BLAST-OFDM system. The number of subcarriers is varied between one and two-hundred and fifty-six. If the correct number of subcarriers is chosen, the performance of both the iterative and original V-BLAST systems can improve, as the delay spread worsens. For each algorithm, approximately eight subcarriers are required to obtain the performance equivalent to that of the coded V-BLAST systems in frequency non-selective block fading channels.

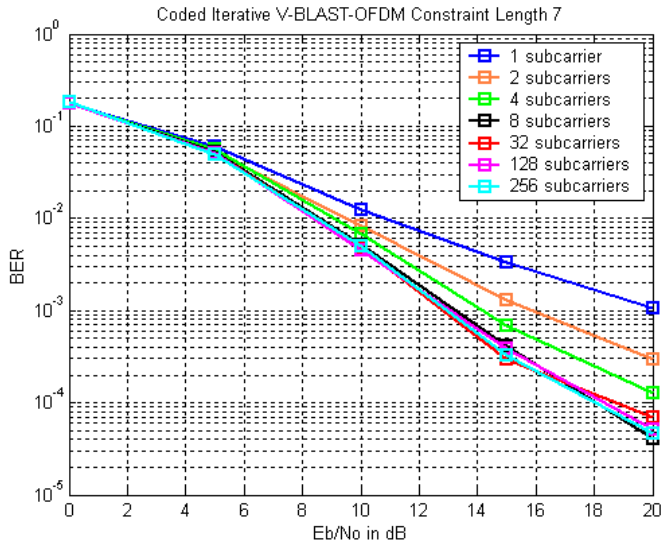

Figure 4.13 Coded Iterative V-BLAST-OFDM System

4.6 Chapter Summary

This chapter analyzed the performance of coded V-BLAST systems. For the quasi-static channel, the combination of convolutional coding with the original V-BLAST algorithm yields no BER performance gain. When the channel is constant over the length of the codeword, the channel decoder is limited by the lack of diversity present in the channel. It was then shown that the combination of convolutional coding with an iterative V-BLAST algorithm provides some coding gain for the same channel conditions.

Six decoding strategies were compared for the iterative V-BLAST algorithm. The best performance was obtained when probability information determined in the iterative V-BLAST algorithm was used as the *a priori* probability information for the BCJR decoding algorithm. Finally, the performance of coded V-BLAST-OFDM systems were considered for quasi-static frequency selective fading channels. Coded V-BLAST-OFDM systems in frequency selective quasi-static channels can achieve performance equivalent to that of coded V-BLAST systems in frequency non-selective block fading channels.

Chapter 5

Channel Estimation Strategies for the Coded Iterative V-BLAST System

5.1 Introduction

In this chapter, several channel estimation strategies are proposed for the iterative V-BLAST algorithm, described in Chapter 4. Strategies for both uncoded and coded systems will be discussed. The only channel model under consideration is frequency non-selective quasi-static fading. Each channel estimation technique discussed requires known pilot symbols to be transmitted at the beginning of each data frame. Pilot symbols reduce spectral efficiency; therefore, it is desirable to use as few as possible. The ultimate objective herein is to achieve performance equivalent to the perfect channel knowledge case by using only N_t pilot symbols.

Some previously suggested channel estimation strategies for MIMO systems include: joint data detection and channel estimation based on the expectation-maximization algorithm [27], [28], [29], overlay pilots [30], pilot embedding [31], and Least Squares estimation (as described in Chapter 3). The above approaches require more than N_t pilot symbols, and can be complex.

One approach that is gaining in popularity is joint data detection and channel estimation. Estimates of the channel and data sequentially improve each other. Combining joint data detection and channel estimation with an iterative algorithm is a logical choice. A simple channel estimator has been proposed that uses estimates of all data symbols within a frame to update the channel estimate [9]. This approach will be shown to outperform

Least Squares estimation; however, it does approach perfect channel knowledge performance.

In this chapter, some simple extensions to the previously proposed joint data detection and channel estimation strategy will be presented for the iterative V-BLAST algorithm. For the uncoded case, reinitializing and repeating the algorithm, after both the channel estimate and data estimate converge, provides performance equivalent to the perfect channel knowledge case at high SNR. The same channel estimation strategies applied to an uncoded system do not yield the same performance enhancements for a coded V-BLAST system. For a coded system, performance is further enhanced by repeating the entire decoding process.

5.2 Channel Estimation Strategies for the Uncoded System

5.2.1 System Model

Throughout the chapter, the examples discussed will be for four transmit and four receive antennas. Additionally, in all examples the channel is quasi-static channel and constant over 400 consecutive time intervals. N_t pilot symbols are transmitted at the beginning of each frame. The pilot symbols make up only 1% of the data frame. The approaches presented could easily be extended to an arbitrary number of transmit antennas, receive antennas, and channel frame length.

5.2.2 Least Square Estimation

The performance of the iterative V-BLAST algorithm is more accurately modeled by removing the perfect channel knowledge assumption. As with the original V-BLAST

algorithm, Least Squares estimation with pilot symbols is a possible channel estimation strategy. Figure 5.1 shows the resulting performance for Least Squares estimation. The number of pilot symbols varies from four to thirty-two pilot symbols per transmit antenna. To be within 1 db of the perfect channel knowledge case, thirty-two pilot symbols per transmit antenna are required. When the channel is estimated with only four pilot symbols per transmit antenna, the performance is approximately 3.5 dB away from the perfect channel knowledge performance.

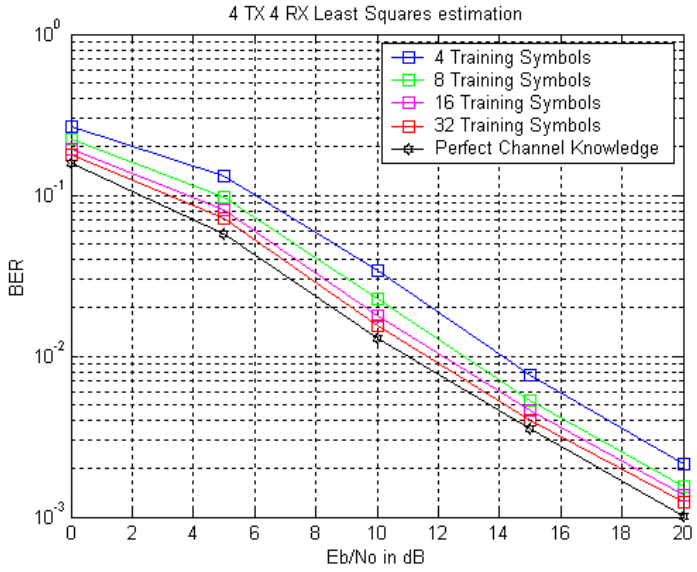

Figure 5.1 Least Squares Estimation with Varying Numbers of Pilot Symbols

Figure 5.2 shows the convergence rate of the iterative V-BLAST algorithm for four orthogonal pilot symbols. As with the perfect channel knowledge case, the algorithm converges after three iterations. At low signal to noise ratio, the additional iterations yield no significant gain.

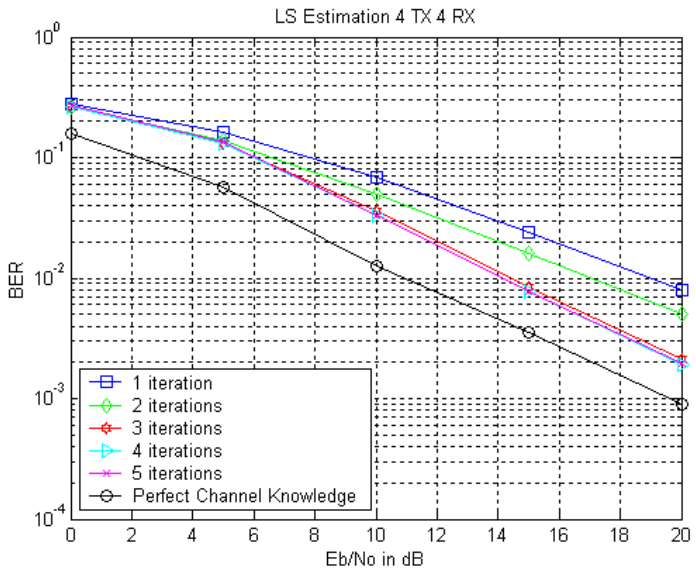

Figure 5.2 Convergence rate of iterative V-BLAST algorithm with four pilot symbols and LS Estimation

5.2.3 Averaged Estimation

Using pilot symbols reduces spectral efficiency. Therefore, it is desirable to use as few pilot symbols as possible. A channel estimator was proposed to sequentially re-estimate the channel [9]. An initial channel estimate is formed from a minimal number of pilot symbols (N_t per transmit antenna). At each time interval, the estimates of all transmitted symbols are used to improve the channel estimate. The channel at time interval *l* can be estimated by

$$\hat{h}_i[l] = conj(\hat{x}_i[l])\left(r[l] - \sum_{i \neq m}^{N_t} \hat{x}_m[l]\tilde{h}_i[l] \right) \tag{5.1}$$

where $\hat{h}_i$ is the estimate of i[th] column of the channel matrix H; $\tilde{h}_i$ is the initial estimate of the i[th] column of H; $\hat{x}_i$ is the estimate of the symbol transmitted from the i[th] transmit antenna; and r is the received signal vector.

Under the quasi-static channel assumption, the channel is constant over many consecutive symbols. The final channel estimate is obtained by averaging all channel estimates obtained in equation 5.1

$$\hat{h}_i = \frac{1}{\|x_i\|^2} \sum_{l=1}^{L} \hat{h}_i[l] \tag{5.2}$$

where L is the number of symbols over which the channel is constant. Although often referred to as 'data aided estimation', this technique is referred to as the averaged estimator in the sequel. An estimate obtained from the pilot symbols is also factored into the averaged estimator.

One iteration of the iterative V-BLAST algorithm is performed, for all received signals within a frame, before moving onto the next iteration. Between iterations of the iterative V-BLAST algorithm, the estimated data sequence can be used with the averaged estimator to improve the channel estimate. In each successive occurrence of the averaged estimator, the previous channel estimate is used as the initial channel estimate in equation 5.1. The new channel estimate is then used to improve the estimates of the data sequence. In each iteration, the new channel estimate is used in the symbol cancellation step (equation 4.2) and the probability calculation (equation 4.4).

Figure 5.3 shows the performance of the averaged estimator as compared to Least Squares Estimation. Four iterations are considered, and the averaged estimator is used to improve the channel estimate after the first, second, and third iteration. Four orthogonal pilot symbols are used to form the initial channel estimate. After four iterations, the averaged estimator outperforms Least Squares estimation by approximately 1 dB.

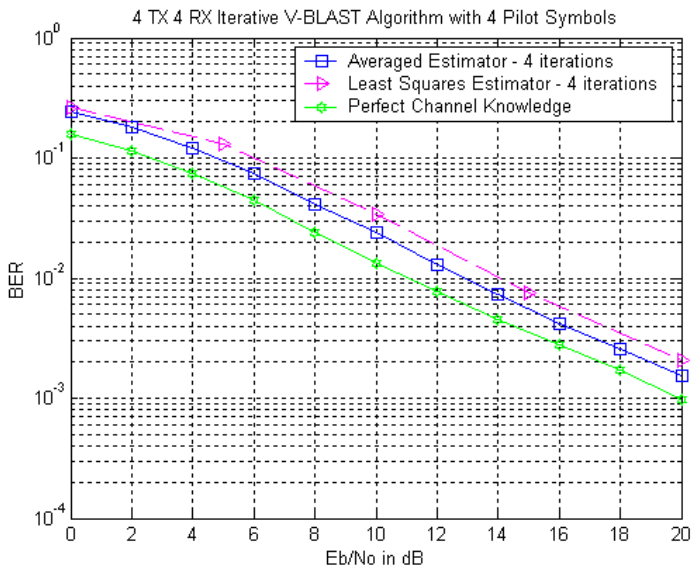

Figure 5.3 Comparison between Least Squares Estimation and the Averaged Estimator

After each execution of the averaged estimator, the updated channel estimate more closely approaches the known channel. Figure 5.4 shows the mean squared error between the channel estimate and the known channel after each iteration. Additionally, figure 5.4 shows the mean squared error for Least Squares estimation with varying numbers of pilot symbols. The estimated data sequence used to update the channel estimate will often have errors. Figure 5.4 shows that even with errors in the estimated data symbols, the averaged estimator still provides a better channel estimate than using only four pilot symbols with Least Squares estimation. The starting point for the averaged estimator is the Least Squares channel estimate. The averaged estimator uses all the estimated data symbols to improve the channel estimate. Furthermore, the averaged estimator can be executed several times. Each execution of the averaged estimator takes advantage of the previously improved channel estimate. For signal to noise ratio greater than 8 dB, after four iterations of the averaged estimator, the channel

estimate is as good as the channel estimate obtained with 32 pilot symbols and least squares estimation.

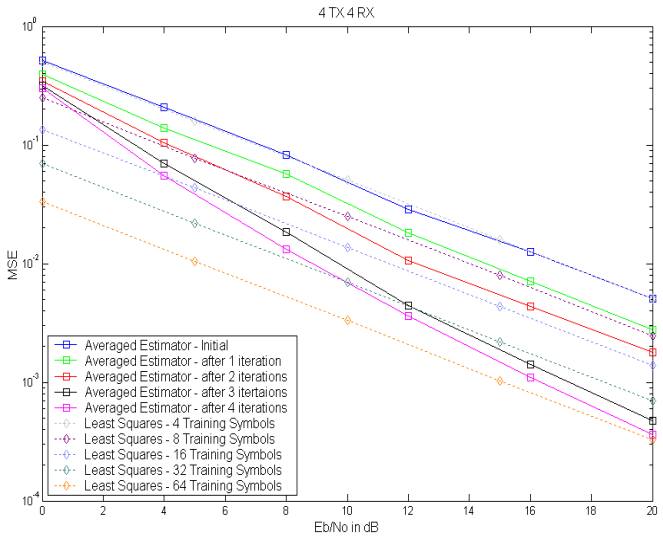

Figure 5.4 MSE of each Iteration for the Averaged Estimator

5.2.4 Pilot Symbols and the Averaged Estimator

The averaged estimator could be used as an alterative to Least Squares estimation. Instead of using all estimated transmitted symbols to estimate the channel, the averaged estimator could be limited to only known pilot symbols. When compared with Least Squares estimation, the averaged estimator requires more symbols to yield an equivalent estimate. Mean squared error (MSE) criterion indicates how close both estimation techniques are to the actual channel matrix **H**. Figure 5.5 shows MSE versus E_b/N_o for one execution of both channel estimation strategies. The averaged estimator requires twelve pilot symbols (including the four used to form the initial channel estimate) to yield yields a channel estimate as good as Least Squares Estimation with eight pilot symbols.

Further, the averaged estimator requires one-hundred total pilot symbols to yield yields a channel estimate as good as Least Squares Estimation with sixty-four pilot symbols.

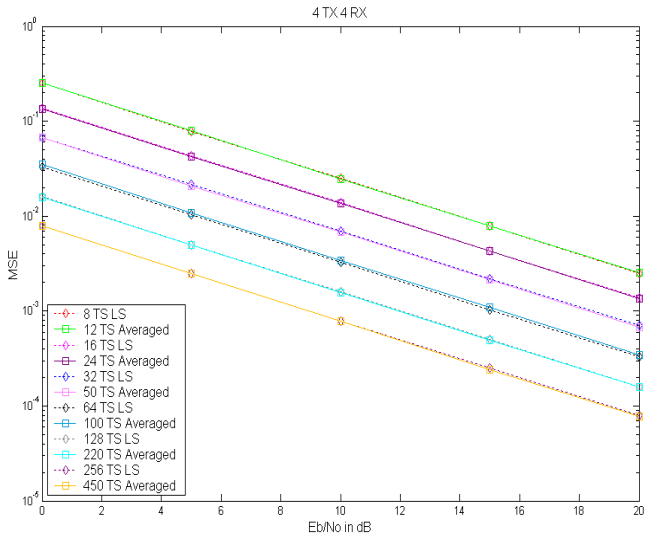

Figure 5.5 MSE Comparisons of Least Squares and Averaged Estimators

The reduced spectral efficiency of the averaged estimator make is a less attractive option than Least Squares Estimation. However, if fewer computations are required, then the averaged estimator might still be a viable option. The number of computations required for each execution of the averaged estimator is $LN_t^2 N_r + LN_t N_R$ multiplications and $LN_t^2 N_r + LN_t(N_r + 1)$ additions. An additional N_t^2 multiplications and N_t^2 additions are required to obtain the initial channel estimate. Table 5.1 compares the complexity of Least Squares Estimation with the averaged estimator.

Table 5.1 Computational Complexity Comparison

Least Squares Estimation		Averaged Estimator		
Number of Pilot Symbols	**Number of Computations**	**Number of Pilot Symbols**	**Number of Computations**	**Difference**
8	896	12	1936	-1040
16	1344	24	3712	-2368
32	4672	50	7560	-2888
64	17472	100	14960	2512
128	67648	220	32720	34928
256	266304	450	66760	199544

For a significantly large number of pilot symbols, the averaged estimator is a good substitute for Least Squares estimation in terms of computational complexity. However, when using the averaged estimator with a small number of pilot symbols, the performance is inferior, and more computations are required when compared with Least Squares.

5.3 Further Improvements

5.3.1 Stopping Criteria

Unnecessary iterations and decoding delay can be avoided by ending the iteration process upon satisfaction of some stopping criterion. Stopping criteria is typically used with turbo decoders, but is employed here between successive iterations of the iterative V-BLAST algorithm. The employment of stopping criteria results in no noticeable performance loss. Two simple stopping criteria are the hard-decision-aided (HDA) and the sign-change-ratio (SCR) stopping rules [32].

The HDA rule states that if hard decisions after two consecutive iterations agree, the decoder stops. The SCR rule compares the ratio of sign changes to an empirical threshold. For example, iterations stop when

$$T(i) \leq (0.005 \sim 0.003)N$$

where N is the number of bits in the frame and T(i) is the number of sign changes between successive iterations.

5.3.2 Reinitializing the Algorithm

The performance of the iterative V-BLAST algorithm can be further improved by reinitializing the algorithm after the channel estimate and estimated data sequence have converged. Each iteration of the iterative V-BLAST algorithm uses information from previous iterations to update the estimated data sequence. Reinitializing the algorithm provides a fresh start for symbols that wrongly converged due to poor channel estimate.

Figure 5.6 shows the performance of the iterative V-BLAST algorithm. Stopping criteria prevents unnecessary iterations. The averaged estimator is executed between iterations and the algorithm is reinitialized after four iterations. Up to four additional iterations are allowed after reinitialization. The channel estimate is not updated after re-initialization. For signal to noise ratios greater than 10 dB, reinitializing the algorithm provides performance equivalent to that of the perfect channel knowledge case. For signal to noise ratios in the range of 4-10 dB, reinitializing the algorithm provides about ½ - 1 dB of gain over the performance of the averaged estimator without reinitializing.

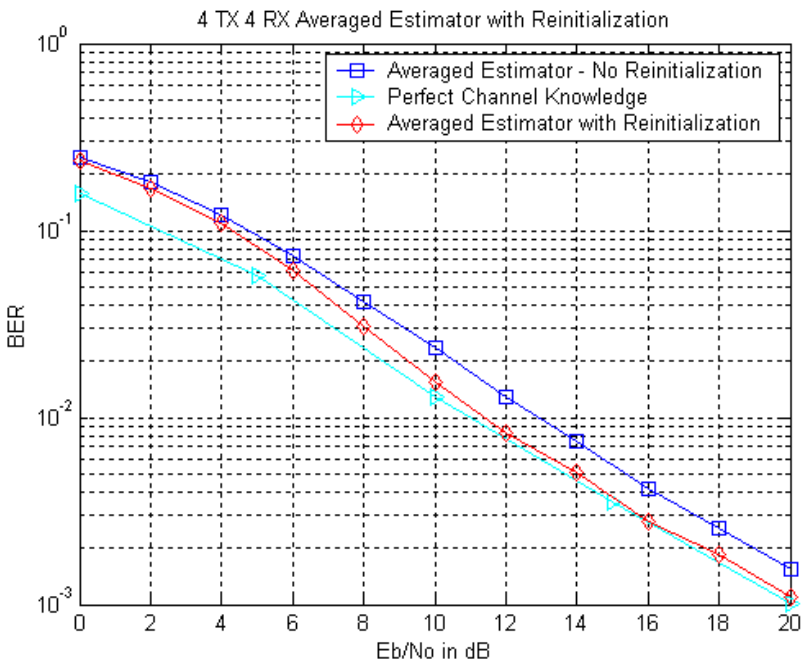

Figure 5.6 Iterative V-BLAST Algorithm with Reinitialization.

Figure 5.7 shows the number of iterations versus E_b/N_o for the HDA stopping rule. The maximum number of iterations is eight; four before and four after reinitializing. Stopping criteria saves the most iterations at mid to high signal to noise ratio. On average, the iterative process stops before reinitializing at high signal to noise ratio. Stopping criteria provides flexibility; extra iterations are available when the algorithm converges slowly.

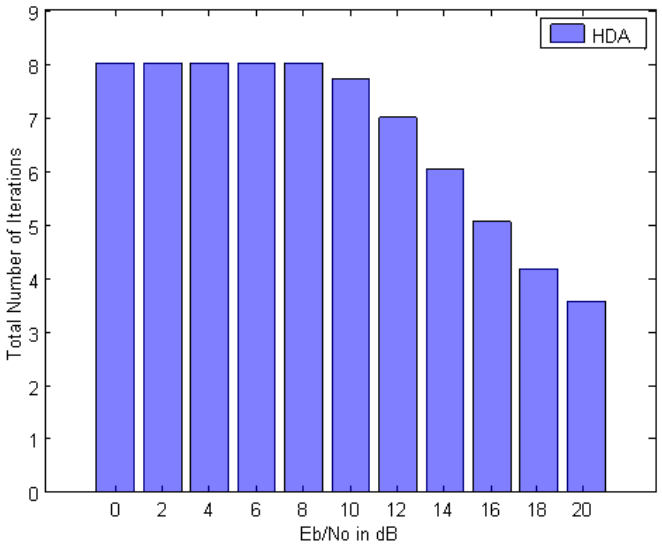

Figure 5.7 Total Number of Iterations

For signal to noise ratio greater than 10 dB, the above approach yields performance almost identical to that of the perfectly known channel case. However, for signal to noise ratio less than 10 dB, there is still room for improvement. Errors in the estimated data sequence, used to update the channel estimate, limit the performance at low signal to noise ratio.

5.3.3 Idealized Case

For the averaged estimator, the improved channel estimates are limited by errors in the estimated data symbols. The performance at low signal to noise ratio should improve if only correct intervals are used to update the final channel estimate before reinitialization. Correct intervals are those time intervals where the estimated symbols from all transmit antennas have been correctly estimated. Prior to reinitializing the algorithm, if it were known which intervals were correct, those intervals could be treated as new pilot symbols. The new pilot symbols could be used with the averaged estimator to obtain a

final channel estimate. Figure 5.8 shows the performance potential of this idealized scenario. Figure 5.9 summarizes the average number of correct intervals after four iterations for given E_b/N_o. At high signal to noise ratio, there is an average of more than 350/400 correct intervals. Estimating the channel with only the new pilot symbols provides no significant improvement compared with using all received symbols at high signal to noise ratio. For low signal to noise ratio, using only the correct intervals provides the potential for only ½ dB improvement as compared with using all intervals to estimate the channel. At low signal to noise ratio, when the channel estimate is updated with only correct symbols, the performance is still 2 dB away from the perfectly known channel case.

There are two possible explanations as to why the performance increase potential is not greater at low signal to noise ratio. First, after four iterations, there is an average of 50-200 correct intervals. Fifty or more intervals should be enough to achieve channel estimates close to the actual channel. However, fifty is the merely the average; sometimes much fewer are correct. Another reason for poor performance at low signal to noise ratio is that that correct intervals do not always provide the most valuable channel information. The correct intervals often include symbols that would not have been correctly estimated with perfect channel knowledge. At low signal to noise ratio, the symbols that are actually correct are sometimes helped, instead of hindered, by the poor channel estimate or noise. As a result, the correct symbols may not help determine the actual channel.

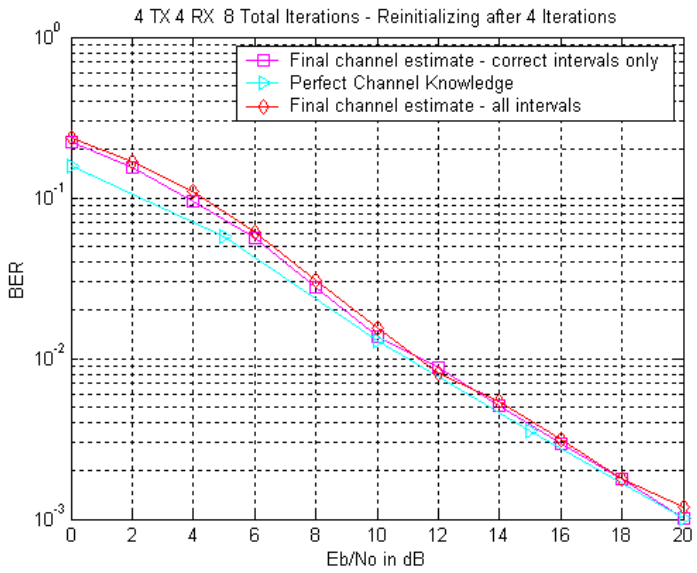

Figure 5.8 Performance potential for using only Correct Intervals.

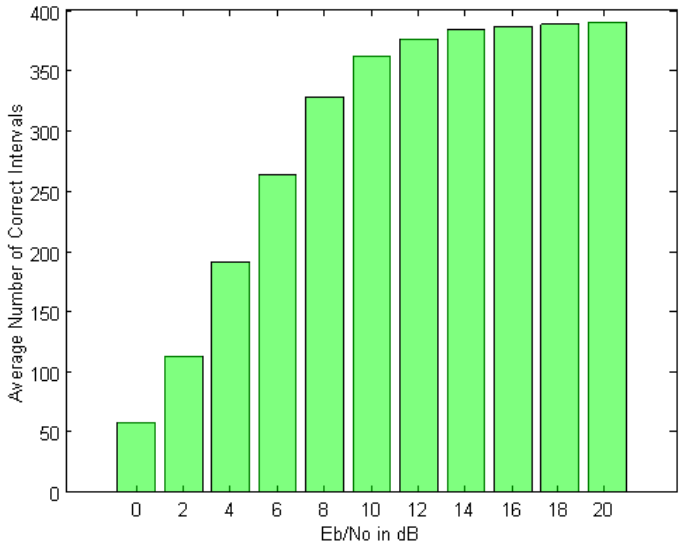

Figure 5.9 Average Number of Correct Intervals.

For the final channel estimate, the averaged estimator was initially chosen to reduce computational complexity for a large number of pilot symbols. At low signal to noise ratio, the performance may be further enhanced when Least Squares estimation is used as the channel estimator. Figure 5.10 shows the idealized performance potential when only

the new pilot symbols estimate the channel with Least Squares estimation. For less than 4 dB, the potential performance improvement of Least Squares estimation compared with the averaged estimator is negligible. For the range of 4-9 dB, when estimating the channel with only correct intervals, Least Squares Estimation has possible advantage over the averaged estimator by only ½ dB.

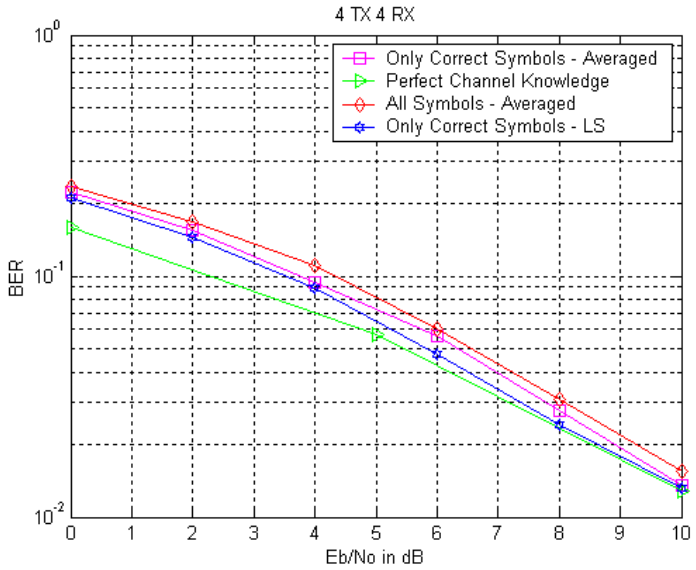

Figure 5.10 Comparison between Least Squares Estimation and the averaged Estimator for the Idealized Case.

The idealized case assumes that it is possible to determine which intervals are correct. The estimates of all transmitted symbols for a given time interval must be correct to be a correct interval. The probability information determined in the iterative V-BLAST algorithm could be used to estimate which intervals are correct intervals. However, determining which intervals are actually correct at low signal can be complicated. At low signal to noise ratio there are many false positives – symbols with very high probabilities that are not actually correct. The false positives occur due to the poor channel estimates used in the iterative algorithm. Another source of inaccurate estimates is when one

symbol with low probability is overshadowed by stronger symbols. Estimating the channel with only the correct intervals provides a maximum improvement of less than 1 dB. The limited increase in performance potential, and the corresponding difficulty in determining which symbols are most correct, makes using only the correct symbols not a viable option.

5.4 Channel Estimation for Coded Iterative V-BLAST Algorithm

When the perfect channel knowledge assumption is removed from the coded iterative V-BLAST algorithm, the performance must be reexamined. The system model is the same as for the uncoded case. The soft decision BCJR algorithm decodes the constraint length seven convolutional code. Probability information from the iterative V-BLAST algorithm is used as the *a priori* probability in the BCJR algorithm. Techniques similar to those employed in the uncoded system can be used for the coded system. Figure 5.11 shows the performance of the coded iterative V-BLAST algorithm with the averaged estimator. Additionally, figure 5.11 shows the performance for perfect and idealized re-initialization after four iterations. Reinitializing the algorithm after the final channel estimate, determined from only the correct intervals, yields the best performance. However, the performance is still approximately 2 dB away from the perfectly known channel case.

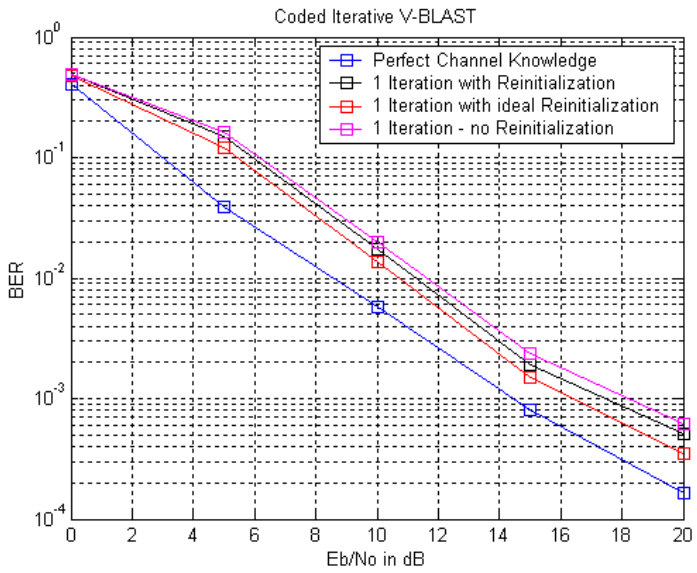

Figure 5.11 Least Squares Estimation, Averaged Estimation, and Reinitialization

The performance of the coded iterative V-BLAST system can be further enhanced by repeating the entire decoding process. Figure 5.12 illustrates the decoding process. The decoded data is used to generate an estimate of the transmitted data sequence. Before the second decoding cycle, this estimate of the transmitted data sequence is used with the averaged estimator to generate another improved channel estimate.

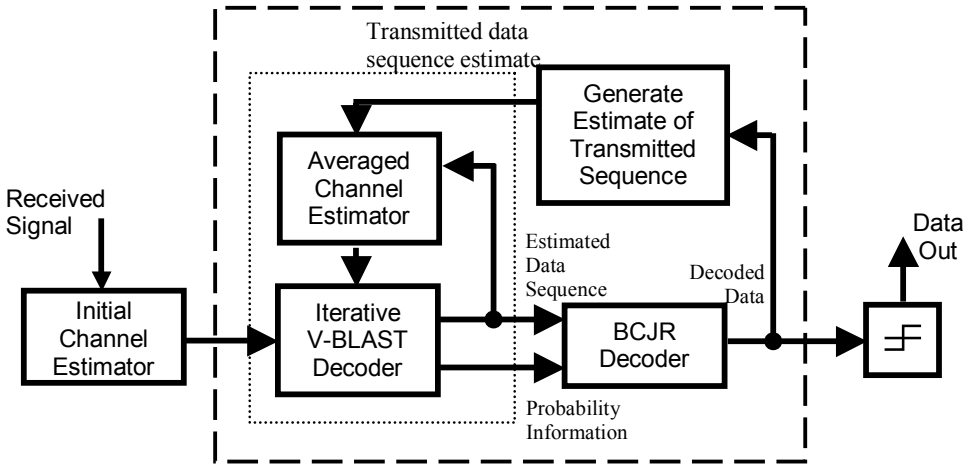

Figure 5.12 Decoding Process for Coded Iterative V-BLAST System.

A possible variation of the above procedure is to not reinitialize the algorithm in either the first, second, or both decoding cycles. Another variation is to use the transmitted sequence estimate as the starting point for the first iteration of the iterative V-BLAST algorithm (second time through). Yet another variation is to not use the averaged estimator in the second decoding cycle. The channel estimate from the transmitted sequence estimate is used as the final estimate.

In addition to employing a stopping criteria within the iterative-V-BLAST algorithm, stopping criteria can also be used to prevent unnecessarily repeating the entire decoding process. When the transmitted sequence estimate, determined after convolutional decoding, is equal to the data sequence used to decode the convolutional code, then the decoding procedure is not repeated.

The basic decoding procedure can be summarized as follows:

1. Obtain an initial channel estimate
2. Iterative V-BLAST algorithm – using averaged channel estimator to update channel estimate – four iterations
3. Reinitialize iterative V-BLAST algorithm – up to four more iterations (optional)
4. Decode convolutional code – soft decision BCJR algorithm with a priori probability information
5. Generate estimate of transmitted sequence from decoded data – re-estimate channel
6. Stopping criteria check point – if data before and after BCJR decoding is same, procedure is stopped
7. Repeat steps 2-4

Repeating the decoding procedure for the perfect channel knowledge case provides no additional gain. Even when the transmitted sequence estimate is the starting point for the second decoding cycle, there is not enough new information available to change the overall system performance.

Figure 5.13 shows simulation results for two decoding cycles of the coded iterative V-BLAST algorithm, without perfect channel knowledge. The four different variations of the decoding process that were tested can be summarized as follows

1. First decoding cycle – up to eight iterations, reinitializing after four iterations. Second decoding cycle – up to four iterations, no reinitializing.
2. First decoding cycle – up to eight iterations, reinitializing after four iterations. Second decoding cycle – up to four iterations – no reinitializing - no averaged estimator.
3. First decoding cycle – up to eight iterations, reinitializing after four iterations. Second decoding cycle – up to eight iterations, reinitializing after four iterations, estimated transmitted sequence used to initialize second decoding cycle.
4. First decoding cycle – up to four iterations – no reinitializing. Second decoding cycle – up to four iterations – no reinitializing.

All variations considered outperform the performance obtained after only one decoding cycle. The best performance is obtained when the estimated transmitted data sequence is used to initialize the second decoding cycle (variation number 3). After approximately 10 dB, the performance was equivalent to that of the perfect channel knowledge case. For high signal to noise ratio, the simplest option (variation number 4) still obtained performance close to the perfectly known channel case.

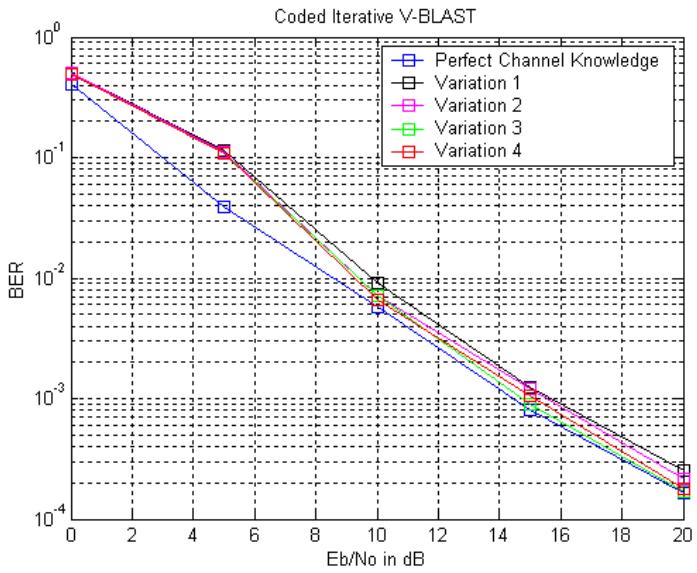

Figure 5.13 Performance of Variations of Coded Iterative V-BLAST System with Two Decoding Cycles.

Figure 5.14 shows the mean squared error between the various channel estimates and the actual channel matrix for all four variations. Figure 5.14 shows the mean squared error for the initial channel estimate, the final channel estimate used in the first decoding cycle, the channel estimate obtained from the estimated transmitted sequence, and the final channel estimate used in the second decoding cycle. For variations one and two, the final channel estimates from the second decoding cycle are slightly worse than the channel estimate determined from the estimated transmitted data sequence. This indicates that updating the channel in the second decoding cycle is probably unnecessary. Even though the final channel estimate may not be the best channel estimate, the performance is still better than a system executing only one decoding cycle. The convolutional code is more powerful than the V-BLAST decoder. On average, there are fewer bit errors in the estimated data sequence than either executions of the V-BLAST decoder. However, after the second execution of the V-BLAST decoder, there are still fewer bit errors present

than after the first execution. Furthermore, the completion of both decoding cycles leads to the fewest bit errors.

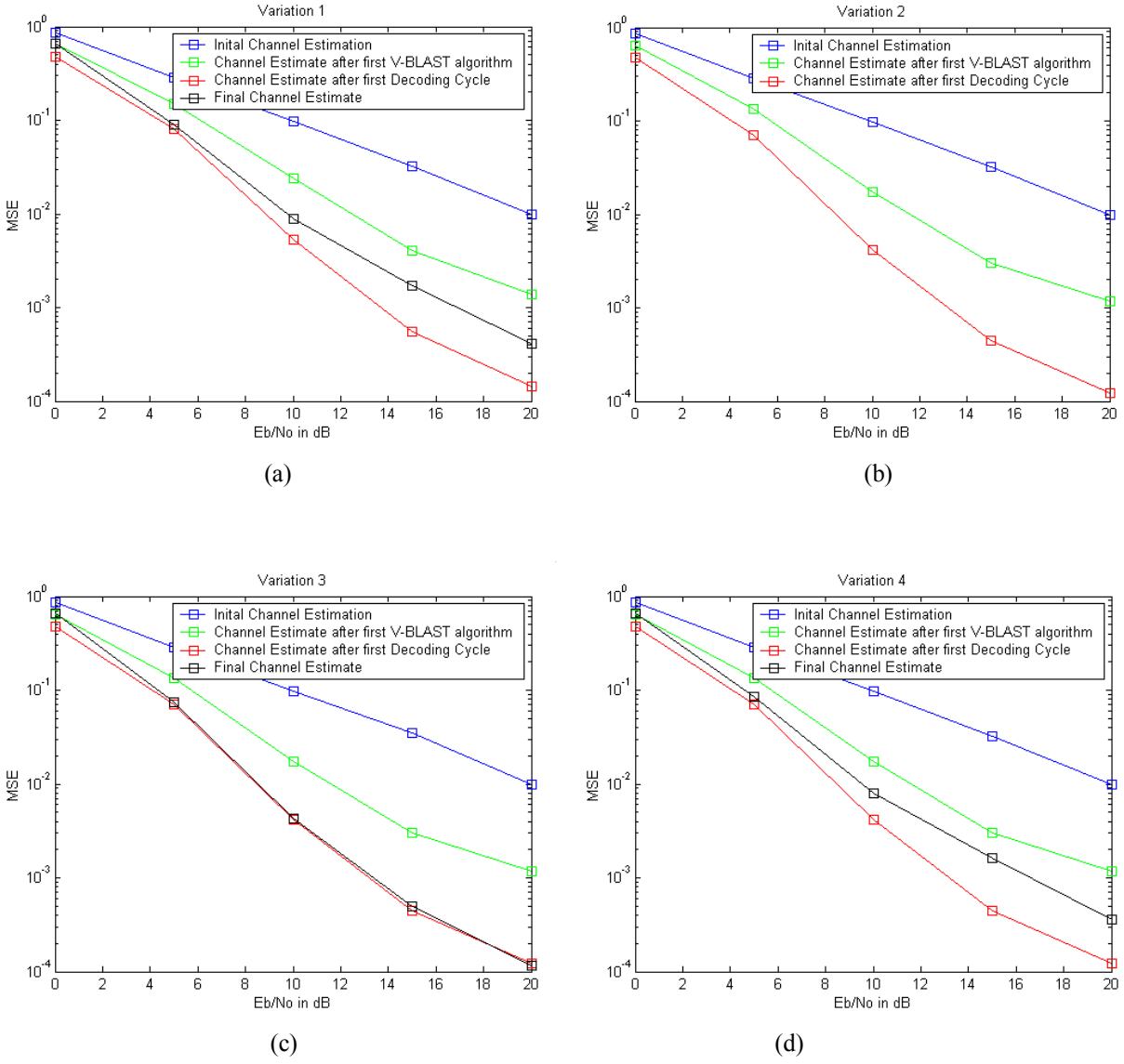

Figure 5.14 Mean Squared Error Between Channel Estimates and Known Channel.(a) Variation 1. (b) Variation 2. (c) Variation 3. (d) Variation 4.

Figure 5.15 shows the average number of total iterations for both decoding cycles of the iterative V-BLAST algorithm. For signal to noise ratios greater than 10 dB, employing stopping criteria significantly reduces unnecessary iterations for all variations. Figure 5.16 shows the average number of decoding cycles. At high signal to noise ratio, when

only four iterations are allowed for the first decoding cycle, the average number of decoding cycles is slightly higher than when eight iterations are allowed for the first decoding cycle.

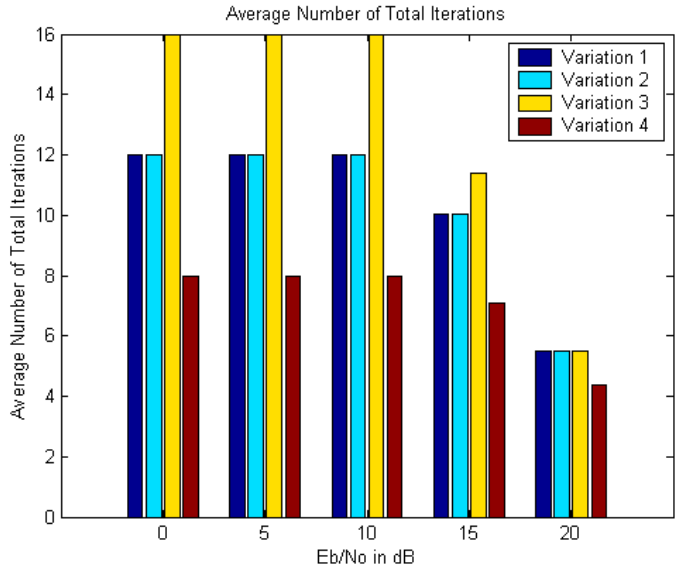

Figure 5.15 Average Number of Total Iterations

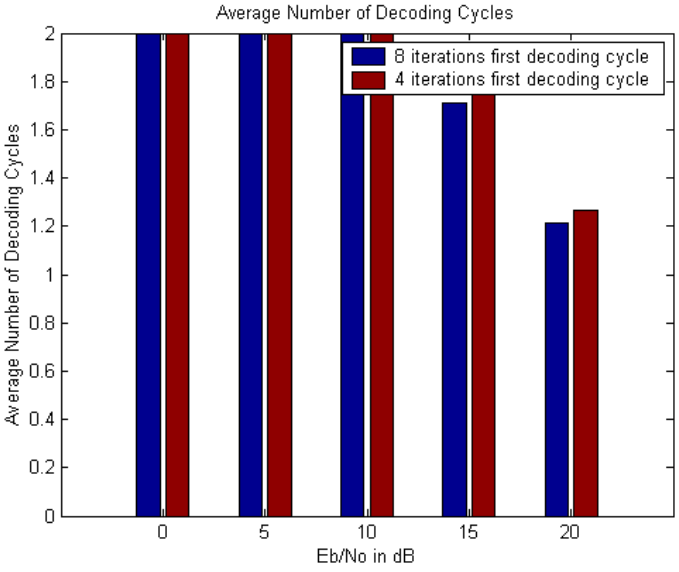

Figure 5.16 Average Number of Decoding Cycles

5.5 Chapter Summary

In this chapter, channel estimation techniques were proposed for the coded and uncoded iterative V-BLAST algorithm. With only N_t pilot symbols, the performance was shown to approach the perfect channel knowledge case at high signal to noise ratio. Between iterations of the iterative V-BLAST algorithm, the channel estimate is updated from all estimated data symbols. After the iterative algorithm and channel estimate have converged, the iterative V-BLAST algorithm is reinitialized using the final channel estimate.

For an uncoded system, the performance at high signal to noise ratio is almost identical to that of a system with perfect channel knowledge. For mid to low signal to noise ratio, the system performance could be slightly enhanced by updating the channel estimates with only the correct intervals. However, it was also shown that at low signal to noise ratio it is difficult to determine which intervals are correct.

The procedure used for the uncoded system does not achieve as good of results when used for the coded system. The performance can be improved by repeating the entire decoding process after obtaining a final channel estimate. The best performance is obtained when the estimated transmitted data sequence is used to initialize the second decoding cycle. However, the simpler approach that requires two decoding cycles, fewer iterations, and no reinitializing yields performance almost equivalent to the perfect channel knowledge case.

In this chapter, it has been shown that close to perfect channel knowledge can be obtained while transmitting only a minimal number of pilot symbols for coded and uncoded systems. However, the increase in complexity and decoding delay may overshadow the

gain in spectral efficiency. In a low signal to noise ratio environment, none of the proposed approaches provide significant performance improvements. The best option for low signal to noise ratio is probably the use of more pilot symbols.

Chapter 6

Conclusion

6.1 Summary of Results

Chapter 2 describes the two main space-time coding techniques; Space-Time Block Codes and Space-Time Trellis Codes. Additionally, Chapter 2 examines the performance of a concatenated Space-Time Block Code-Trellis Coded Modulation system. The performance of the concatenated STBC-TCM system and the STTC system were analyzed for quasi-static and block fading channel models. The quasi-static channel was shown to inhibit the BER performance potential of the STBC-TCM system

Chapter 3 describes the basic principles and original detection procedure for V-BLAST architecture. The effect of the error propagation problem that results from the successive interference cancellation was examined for the V-BLAST architecture. Finally, the system performance was examined when Least Squares and MAP Estimation were used to estimate unknown channel characteristics.

Chapter 4 examines the performance of coded V-BLAST systems. Similar to the STBC-TCM systems described in Chapter 2, the addition of coding can hinder the BER performance in the quasi-static fading channel. An iterative soft interference cancellation V-BLAST algorithm was presented as an alterative to the original V-BLAST algorithm. The iterative algorithm was originally proposed to alleviate the error propagation effects present in the original V-BLAST algorithm. Combining coding with the iterative V-BLAST algorithm improved system performance. Finally, Chapter 4 describes a coded V-BLAST-OFDM system for frequency selective quasi-static fading channels. For both

the original and iterative V-BLAST algorithm, the coded V-BLAST-OFDM system obtains the same performance as the frequency non-selective block fading channel.

Chapter 5 proposes several channel estimation strategies for the iterative V-BLAST system. The channel estimate can be sequentially improved between successive iterations of the V-BLAST algorithm. For both the coded and uncoded systems at high signal to noise ratio, only N_t pilot symbols per transmit antenna are required to achieve perfect channel knowledge performance.

6.2 Future Work

This section describes some possible extensions to the research presented in this thesis.

1. In this thesis, it was shown that for coded MIMO systems where the quasi-static channel is constant over the same interval as the codeword, the system may not benefit from the addition of coding. The system performance improves when the quasi-static channel is transformed into a block fading channel. Another possible solution is to change the detection strategy of the inner system. A topic of further research involves exploring channel codes and channel decoding strategies that might be less sensitive to the lack of diversity in the quasi-static channel environment.
2. This thesis proposed channel estimation strategies for the frequency non-selective quasi-static slow Rayleigh fading channel. In the future, the strategies proposed could be applied to the coded iterative V-BLAST-OFDM system. Additionally, the techniques presented could be extended to estimate time-varying channels.

3. A final suggestion for future investigation is to improve the channel estimation procedure at low signal to noise ratio. For both uncoded and coded systems, it may be possible to obtain the perfect channel knowledge performance at low signal to noise ratio with only N_t pilot symbols.

Bibliography

[1] Foschini GJ, Gans MJ. On limits of wireless communications in a fading environment when using multiple antennas. *Wireless Personal Communications, vol.6, no.3, March 1998, pp.311-35. Publisher: Kluwer Academic Publishers, Netherlands.*

[2] Alamouti SM. A simple transmit diversity technique for wireless communications. *IEEE Journal on Selected Areas in Communications, vol.16, no.8, Oct. 1998, pp.1451-8. Publisher: IEEE, USA.*

[3] Tarokh V, Seshadri N, Calderbank AR. Space-time codes for high data rate wireless communication: performance criterion and code construction. *IEEE Transactions on Information Theory, vol.44, no.2, March 1998, pp.744-65. Publisher: IEEE, USA.*

[4] G.J. Foschini, "Layered space-time architecture for wireless communication in a fading environment when using multi-element antennas". *Bell Labs Technical Journal, 1996.*

[5] Xuan Chi, *The Impact of Channel Estimation Error on Space-Time Block and Trellis Codes in Flat and Frequency Selective Channels. M.S. Thesis.* Virginia Poly. Inst. and State University, 2002.

[6] Rekha Menon, *Impact of Channel Estimation Errosr on Space-Time Trellis Codes. M.S. Thesis.* Virginia Poly. Inst. and State University, 2003.

[7] Hassibi B, Hochwald BM. How much training is needed in multiple-antenna wireless links? *IEEE Transactions on Information Theory, vol.49, no.4, April 2003, pp.951-63. Publisher: IEEE, USA*

[8] Won-Joon Choi, Kok-Wui Cheong, Cioffi JM. Iterative soft interference cancellation for multiple antenna systems. *2000 IEEE Wireless Communications and Networking Conference. IEEE. Part vol.1, 2000, pp.304-9 vol.1. Piscataway, NJ, USA.*

[9] Grant A. Joint decoding and channel estimation for space-time codes. *Vehicular Technology Conference Fall 2000. IEEE VTS Fall VTC2000. 52nd Vehicular Technology Conference. IEEE. Part vol.1, 2000, pp.416-20 vol.1. Piscataway, NJ, USA.*

[10] J.G. Proakis, *Digital Communications.* McGraw Hill, 2000.

[11] Gamal HE, Hammons AR Jr. On the design of algebraic space-time codes for MIMO block-fading channels. *IEEE Transactions on Information Theory, vol.49, no.1, Jan. 2003, pp.151-63. Publisher: IEEE, USA.*

[12] Tarokh V, Jafarkhani H, Calderbank AR. Space-time block coding for wireless communications: performance results. *IEEE Journal on Selected Areas in Communications, vol.17, no.3, March 1999, pp.451-60. Publisher: IEEE, USA.*

[13] Ungerboeck G. Channel coding with multilevel/phase signals. *IEEE Transactions on Information Theory, vol.IT-28, no.1, Jan. 1982, pp.55-67. USA.*

[14] Alamouti SM, Tarokh V, Poon P. Trellis-coded modulation and transmit diversity: design criteria and performance evaluation. *ICUPC '98. IEEE 1998 International Conference on Universal Personal Communications. Conference Proceedings. IEEE. Part vol.1, 1998, pp.703-7 vol.1. New York, NY, USA.*

[15] Weimin Zhang, "Finite state systems in mobile communications," Ph.D. Dissertation, *Uni. of South Australia*, Feb. 1996.

[16] Chen Z, Vucetic BS, Yuan J, Ka Leong Lo. Space-time trellis codes for 4-PSK with three and four transmit antennas in quasi-static flat fading channels. *Communications Letters, vol.6, no.2, Feb. 2002, pp.67-9. Publisher: IEEE, USA.*

[17] Abdool-Rassool B, Heliot F, Revelly L, Nakhai R, Aghvami H. 4-PSK space-time trellis codes with five and six transmit antennas for slow Rayleigh fading channels. *Electronics Letters, vol.39, no.3, 6 Feb. 2003, pp.297-9. Publisher: IEE, UK.*

[18] Gong Y, Letaief KB. Concatenated Space-Time Block Coding with Trellis Coded Modulation in Fading Channels. *IEEE Transactions on Wireless Communications, vol.1,no.4, October 2002, pp.580-90. Publisher: IEEE,USA.*

[19] R. Gozali, *Space time codes for high data rate wireless communications. Ph.D Dissertation.* Virginia Poly. Inst. and State University, 2002.

[20] Kyungchun Lee, Joohwan Chun. On the interference nulling operation of the V-BLAST under channel estimation errors. *2002 IEEE 56th Vehicular Technology Conference Proceedings (Cat. No.02CH37359). IEEE. Part vol.4, 2002, pp.2131-5 vol.4. Piscataway, NJ, USA.*

[21] Ben Noble, James W. Daniel, *Applied Linear Algebra*, Prentice-Hall International, 1988.

[22] Xinmin Deng, Alexander M. Haimovich, Javier Garcia-Frias. Decision Directed Iterative Channel Estimation for MIMO Systems. *ICC '03. IEEE International Conference on, Vol.4, Iss., 11-15 May 2003 pp.2326-2329.*

[23] Li X, Huang H, Foschini GJ, Valenzuela RA. Effects of iterative detection and decoding on the performance of BLAST *Globecom '00 - IEEE. Global Telecommunications Conference. Conference Record. IEEE. Part vol.2, 2000, pp.1061-6 vol.2. Piscataway, NJ, USA.*

[24] Bahl LR, Cocke J, Jelinek F, Raviv J. Optimal decoding of linear codes for minimizing symbol error rate. *IEEE Transactions on Information Theory, vol.IT-20, no.2, March 1974, pp.284-7. USA.*

[25] G. L. Stuber, J. Barry, S. McLaughlin, Y. (G.) Li, M. A. Ingram, and T. Pratt, Broadband MIMO-OFDM wireless communications. *Proceedings of the IEEE, Vol.92, Iss.2, Feb. 2004, pp. 271- 294.*

[26] Boubaker N, Letaief KB, Murch RD. A layered space-time coded wideband OFDM architecture for dispersive wireless links. *Proceedings. Sixth IEEE Symposium on Computers and Communications. IEEE Comput. Soc. 2001, pp.518-23. Los Alamitos, CA, USA.*

[27] Boutros JJ, Boixadera F, Lamy C. Bit-interleaved coded modulations for multiple-input multiple-output channels. *2000 IEEE Sixth International Symposium on Spread Spectrum Techniques and Applications. ISSTA 2000. Proceedings. IEEE. Part vol.1, 2000, pp.123-6 vol.1. Piscataway, NJ, USA.*

[28] Yingxue Li, Georghiades CN, Garng Huang. Iterative maximum-likelihood sequence estimation for space-time coded systems. *IEEE Transactions on Communications, vol.49, no.6, June 2001, pp.948-51. Publisher: IEEE, USA.*

[29] Cozzo C, Hughes BL. Joint channel estimation and data detection in space-time communications. *IEEE Transactions on Communications, vol.51, no.8, Aug. 2003, pp.1266-70. Publisher: IEEE, USA.*

[30] Jungnickel V, Haustein T, Jorswieck E, Pohl V, von Helmolt C. Performance of a MIMO system with overlay pilots. *GLOBECOM'01. IEEE Global Telecommunications Conference. IEEE. Part vol.1, 2001, pp.594-8 vol.1. Piscataway, NJ, USA.*

[31] Haidong Zhu, Farhang-Boroujeny B, Schlegel C. Pilot embedding for joint channel estimation and data detection in MIMO communication systems. *Communications Letters, vol.7, no.1, Jan. 2003, pp.30-2. Publisher: IEEE, USA.*

[32] Shao RY, Shu Lin, Fossorier MPC. Two simple stopping criteria for turbo decoding. *IEEE Transactions on Communications, vol.47, no.8, Aug. 1999, pp.1117-20. Publisher: IEEE, USA.*

Vita

Rose Trepkowski was born on September 23, 1979 in Columbus, Ohio. She graduated magna cum laude with a Bachelor's degree in Electrical Engineering from The University of Toledo in May 2002. Currently, Rose is a Bradley Fellow in the Bradley Department of Electrical and Computer Engineering at Virginia Tech. She has been working with Dr. Brian Woerner in the area of multiple antenna systems. Beginning summer 2004, Rose will be working at The Johns Hopkins University Applied Physics Laboratory in Laurel, Maryland.